Recent advances in ultrasound-triggered drug delivery through lipid-based nanomaterials

Amirhossein Ahmadi[1], Samira Hosseini-Nami[2], Ziaeddin Abed[2], Jaber Beik[2], Liliana Aranda-Lara[3], Hadi Samadian[4], Enrique Morales-Avila[5], Mehid Jaymand[4] and Ali Shakeri-Zadeh[6]

[1] Pharmaceutical Sciences Research Center, Faculty of Pharmacy, Mazandaran University of Medical Sciences, Sari 48175-861, Iran
[2] Finetech in Medicine Research Center, Iran University of Medical Sciences (IUMS), Tehran, Iran
[3] Laboratorio de Investigación Teranóstica, Facultad de Medicina, Universidad Autónoma del Estado de México, Toluca, 50180 Estado de México, Mexico
[4] Nano Drug Delivery Research Centre, Health Technology Institute, Kermanshah University of Medical Sciences, Kermanshah 67144 15153, Iran
[5] Laboratorio de Toxicología y Farmacia, Facultad de Química, Universidad Autónoma del Estado de México, Toluca, 50120 Estado de México, Mexico
[6] Institute for Cell Engineering, The Johns Hopkins University School of Medicine, Baltimore, MD 21205-1832, USA

Dr. Amihossein Ahmadi was awarded a Pharm.D from the Faculty of Pharmacy, Mazandaran University of Medical Sciences, Sari, Iran in 2010. He got a scholarship position from National Elites Foundation of Iran to continue his education in Ph.D of radiopharmacy;however, he would like to get his Ph.D from an international prestigious university. He has worked as a researcher in the Pharmaceutical Sciences Research Center of Mazandaran University of Medical Sciences since 2010. He has a demonstrated history of research in pharmaceutical sciences. His research interests include the broad fields of Pharmacology and Toxicology, natural products, nano-radiopharmaceuticals, nanomedicine, and cancer chemoradiotherapy.

The high prescribed dose of anticancer drugs and their resulting adverse effects on healthy tissue are significant drawbacks to conventional chemotherapy (CTP). Ideally, drugs should have the lowest possible degree of interaction with healthy cells, which would diminish any adverse effects. Therefore, an ideal scenario to bring about improvements in CTP is the use of technological strategies to ensure the efficient, specific, and selective transport and/or release of drugs to the target site. One practical and feasible solution to promote the efficiency of conventional CTP is the use of ultrasound (US). In this review, we highlight the potential role of US in combination with lipid-based carriers to achieve a targeted CTP strategy in engineered smart drug delivery systems.

Introduction

Cancer is a complicated, cryptic, multifactorial disease and, according to a report from the American Cancer Society (ACS), the second leading cause of death in the USA [1]. Cancer denotes a group of diseases in which cell proliferation is disrupted from the normal state, causing a loss in the ability to differentiate, uncontrolled growth, and occasionally resistance to death [2]. In this context, surgery (SR) and radiotherapy (RT) are the main treatments when the tumor is located in a specific site. When the malignancy systematically involves the patient's body or when both SR or RT cannot be recommended, CTP can be considered as an effective treatment, wherein

Corresponding author:. Samadian, H. (h30samadiyan@gmail.com), Morales-Avila, E. (emoralesav@uaemex.mx), Shakeri-Zadeh, A. (ashaker3@jhu.edu)

https://doi.org/10.1016/j.drudis.2020.09.026

anticancer drugs are injected or administered orally to the patient [3]. Moreover, the combination of three treatment strategies might be required in some situations. In conventional CTP, drugs are systemically distributed throughout the body and are unable to discriminate between healthy and tumor cells. Thus, a high concentration of drugs is required to achieve sufficient therapeutic treatment inside the tumor to enable the therapeutic dose to reach the target site [4]. However, healthy tissues can be injured by the toxic effects of high concentrations of CTP drugs accumulated by unspecific uptake [5,6]. These drawbacks limit the application of conventional CTP and make it an ineffective and noneconomical treatment approach. Therefore, a suitable targeted strategy needs to be adopted to address these issues and ensure that the highest possible drug dosage reaches the target sites while healthy tissues are preserved from the off-target effects [7,8].

The ideal scenario to bring about improvements in CTP is the use of technological strategies for efficient transport, specific, and selective drug release. This includes encapsulation, entrapment, or binding drugs into the carriers in the same manner as a 'Trojan horse'. Using this approach, the drug reaches the target sites with the fewest interactions with healthy cells, thereby leading to diminished adverse effects. Moreover, target drug delivery can circumvent the administration of a high dose to reach the therapeutic index and requires reduced drug dosage administration rather than free drug administration [9–11]. However, it is necessary to address the nonspecific distribution of the carriers. Hence, the next step of drug targeting, after drug containment, is to determine a sophisticated strategy for targeted and controlled drug release [12–14].

Nanotechnology has significant potential for targeted cancer drug delivery [15–17]. A range of nanomaterials with distinct physiochemical properties are available to isolate chemotropic drugs and endow targeted drug delivery [18,19]. Among these nanomaterials, lipid-based nanomaterials (LNMs) have elicited plenty of research attention in the wake of their biocompatibility, easy, processability, and adjustable drug encapsulation efficacy. Moreover, stimuli-responsive carriers can also be constructed from lipids, which are suitable for adjusting the release kinetic under various endogenous and exogenous stimuli. As mentioned earlier, cancer is a complicated disease that necessitates a combination of treatment modalities for an effective outcome. In this regard, the combination of geotargeting with temporal targeting is an emerging strategy for the improvement of therapeutic results. Geotargeting refers to the concept of enabling the intended drug to reach the desired site, whereas temporal targeting denotes the concept of releasing the proposed drug through the carrier at the desired time [20–22]. Both components require the therapy to be incorporated into a well-designed carrier that can overcome biological barriers and reach the site of action while also releasing the loaded therapeutics under specific stimuli. While various passive and active targeting approaches have been developed for the treatment of cancer, only some have been able to reach the clinic. Meanwhile, studies on temporal targeting through stimuli-responsive carriers have resulted in various proposals based on this concept [23,24]. The stimuli can be endogenous, such as specific enzymes, local pH, and redox chemical reactions, or external, such as temperature, light, electrical or magnetic fields, and US [25]. To that end, US has a range of applications in the clinic, such as imaging, physiotherapy, kidney-stone shattering, flow analysis, tumor ablation, and fibroid ablation, among others. More interestingly, it is possible to trigger drug leakage from the responsive carrier through US-induced heat as well as mechanical effects. This concept has provided additional possibilities for targeted cancer therapy [26–28]. Thus, here, we provide a comprehensive review of the combination of lipid-based nanostructures with an US-induced drug release approach.

Targeted therapy of cancer

Nanotechnology provides suitable medical tools that can be adopted for targeting (at the tissue, cellular, or subcellular level) in cancer therapy by either passive and active targeting (Fig. 1), or a physiological/technical approach, that is, triggered drug delivery systems (Fig. 2).

Passive targeting

Under passive targeting, the passive uptake of drugs carriers occurs in solid tumor tissues via the enhanced permeability and retention (EPR) effect, physiochemical properties, and Fick's law of diffusion, which drives the biokinetics of the drug vehicle. The carriers tend to accumulate passively in a tumor, based on several malignancy parameters resulting from its inherent pathological features, including pH level, disorganized and leaky vasculature, production of vascular permeability factors, and ineffective lymphatic drainage [29–31]. It is proposed that the size of the nanoparticles (NPs) has to be between ~10 to several hundred nm to utilize the EPR effect because of the abnormally wide fenestrations in the blood vessels of most solid tumors [32–34].

Active targeting

Complementing passive mechanisms, active targeting refers to carriers that are anchored to various targeting ligands, such as monoclonal antibodies, proteins, peptides, nucleic acid ligands (e.g., aptamers), estrone, hyaluronic acid, transferrin, RGD, cRGD, and small molecules (e.g., folic acid). Indeed, such targeting moieties specifically and selectively bind the carriers to cell receptors and lead to enhanced uptake. In some cases, they also allow

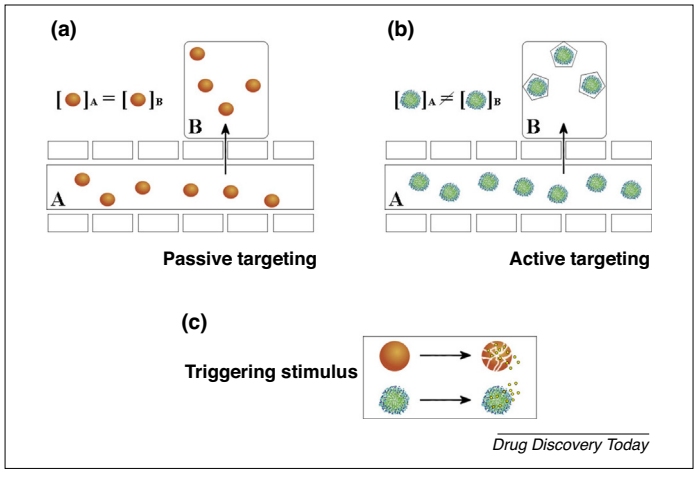

FIGURE 1

Schematic of two physiological ways to target cancer therapy by: (i) passive and (ii) active targeting, using (iii) a targeted stimulus.

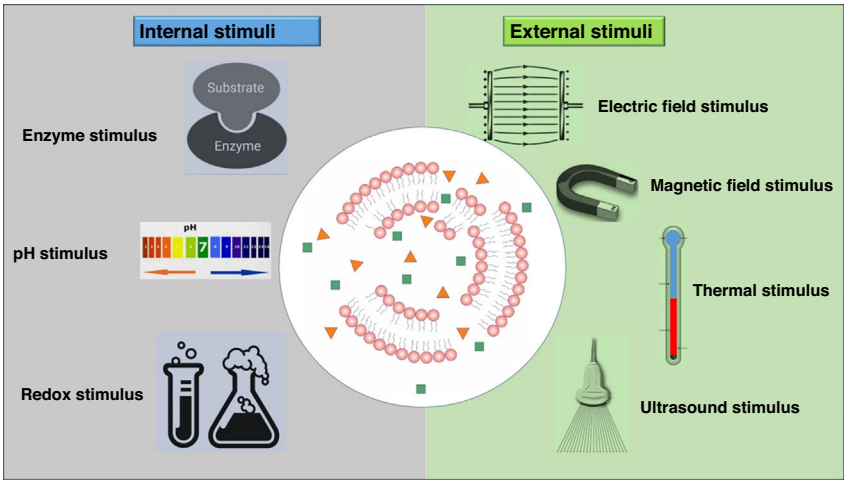

FIGURE 2

Schematic of internal and external stimulations applicable in active drug delivery systems. Internal stimuli include enzyme, pH, and redox stimuli. External stimuli include electric field, magnetic field, thermal, and ultrasound stimuli.

the internalization of NPs or their contents through receptor-mediated endocytosis [18,35–40].

Triggered targeting

Although proper delivery of drug carriers to their targets is a remarkable achievement, an additional mechanism that has the potential to increase the rate of drug release from the carriers at the target site is urgently needed. Indeed, another crucial requirement to meet targeted CTP is a triggering mechanism that provides controlled drug release into the target. A triggering mechanism is defined as a method for adjusting and controlling the span, rate, and compartment of drug release, and is generally categorized as an internal (enzymes, pH, etc.) and external trigger (temperature, laser, ultrasonic waves, alternating magnetic fields, etc.) [41,42]. The advantages and disadvantages of the triggering mechanism are summarized in Table 1 [43–47].

Internal triggers

Enzyme-triggered release utilizes an internal trigger that exploits the inherent pathological features of malignant tissues. The activity of a specific enzyme can be increased at a tumor site, so drug carriers can be designed to be sensitive to that enzyme. For example, liposomes are lipase sensitive because of they contain phospholipids. Strategies based on enzyme-responsive control include matrix metalloproteinases (MMPs), cathepsin B, hyaluronidases, and azoreductases as triggers in anticancer drug delivery [37,48,49]. Another type of internal trigger uses pH-triggered release, which utilizes a class of carriers designed to be responsive to pH changes. These carriers are stable in healthy tissue under normal physiological pH (pH 7.4), but, in the tumor site, where the pH level is more acidic than in healthy tissue (pH~6.5), they become destabilized and release their payloads [50]. Generally, polymers with basic or acidic groups, such as tertiary amines, phosphates, carboxyl, and sulfonic groups, are pH responsive, because these groups are ionizable and induce structural changes alongside pH changes [37,51–53]. Tumors have to reduce intracellular and oxidizing extracellular environments to progress; these environmental changes are beneficial for the development of redox-responsive delivery vehicles. This delivery concept is based on the high cytoplasmic concentration of glutathione tripeptide (2–10 mM) in tumor environments, which can disintegrate the structure of redox-responsive carriers. Disulfide bonds (S–S) are labile in these conditions, making them suitable for the construction of polymer, lipid, peptide, and protein-based delivery systems. Various redox-responsive delivery systems have been developed based on PEG-*S*-*S*-poly(ε-caprolactone), poly(ε-caprolactone), *S*-*S*-poly(ethyl ethylene phosphate), and dextran-*S*-*S*-poly(ε-caprolactone) [8,54–56].

External triggers

External triggers can directly increase the rate of drug release and stimulate internal triggers. For example, US can increase the rate of drug release from carriers directly through its mechanical interactions and indirectly by warming the medium, owing to its thermal interactions. Drug carriers are usually designed to be intact at 37 °C. Thus, increasing the surface temperature of carriers using external triggers (e.g., laser, US, microwaves, alternating magnetic field, etc.) destabilizes them and thereby facilitates drug release [57–61]. Here, we describe the performance of different external triggers. Then, ultrasound-responsive drug-delivery strategies will be reviewed in more detail.

Light-responsive carriers undergo structural changes under interaction with light of a specific wavelength. The radiated light can change the conformation, polarity, hydrophilicity, charge, optical chirality, and conjugation of the carrier, which subsequently alters the shape, stability, wettability, conductivity, solubility, optical properties, and adhesion performance of the polymer [62,63]. Several liposomes have been designed to be photosensitive because of the contribution of light-sensitive lipids in their formulation. [64–66]. In an alternative magnetic field (AMF)-responsive

TABLE 1

Summary of the advantages and disadvantages of the triggering mechanism for drug delivery

Stimuli	Advantages	Disadvantages
Internal triggers		
Enzyme-responsive systems	Protection of drug in blood circulation; tumor-selective accumulation; controlled release of drug; improved pharmacokinetics	Enzyme dysregulations in diseases; heterogeneous spatial and temporal patterns of enzyme activity; substrates overlap for closely related enzyme families; complex large-scale production
pH-Responsive systems	Ease of application; pH differences in human body; controlled drug release; intracellular drug delivery	Not suitable in biosystems when adding acid and base; polymer-related toxicity; low conjugate bioactivity; low mechanical strength
Redox-responsive systems	Stability in normal tissues; prompt response to high GSH concentration (usually a few minutes to hours); drug release in cytoplasm	Heterogeneity of tumor cells; complex biological environment
External triggers		
Light-responsive systems	Very precise; easily tuned; low cost; spatiotemporal control	Limited tissue penetration (can be enhanced with NIR light); invasive for deep zone; UV is harmful; inconsistent responses to light
AMF-responsive systems	Accumulation of particles with magnetic field; energy modulation with alternating magnetic field; Noninvasiveness; High penetration; Spatiotemporal control; Insensitive to surrounding medium	Accumulation can lead to embolism or increased cytotoxicity; complex and high cost; large facilities
Electro-responsive systems	Pulsative release with changes in electric current; spatiotemporal control	Surgical implantation required; requires additional equipment for external application of stimulus; difficulty tp optimize magnitude of electric current; low penetration ability; sensitive to surrounding medium
Thermo-responsive systems	Ease of incorporation of active moieties; simple manufacturing and formulation; achieve light-, US-, and magnetic-induced local heating	Instability of thermolabile drugs; induces environmental changes; damage to biological systems
US	High penetration (dependent on frequency); easily tuned; low cost; ability for very focused heating; insensitive to surrounding medium	Difficulty to target moving organs; homogeneous exposure to large zones remains a challenge; high reflection at air (99%) and bone (60%) interface; high absorption in bone; specialized equipment for controlling drug release

system, a local high-frequency AMF is used to induce hyperthermia in the tumor site and accelerate the release of the drug from the thermosensitive liposome (TSL) carrier. However, a high-intensity AMF needs to be applied, which causes harmful effects in healthy tissues. A solution was recently developed based on the use of magnetoliposomes (MLs) that contain superparamagnetic NPs [67,68]. Halevas *et al.* [69] magnetized ternary V(IV)-curcumin-bipyridine complex-loaded liposomes via the addition of citrate-coated Fe_3O_4 magnetic NPs as the triggered drug delivery system. They showed that the citrate-coated Fe_3O_4 magnetic NPs were loaded into the hydrophilic lumen of the liposome, whereas V(IV)-curcumin-bipyridine was entrapped in the hydrophobic compartment of the lipid bilayer. In another study, Hardiansyah *et al.* [68] synthesized doxorubicin (DOX)-loaded PEGylated liposomes magnetized via the loading of citrate-coated Fe_3O_4 magnetic NPs.

Electroactive organic/inorganic materials can be exploited to fabricate stimuli-responsive delivery systems. Electrically induced redox reactions and the orientation of the dipoles under the applied electric field are the main underlying mechanisms of electro-responsive delivery systems. Different electroactive materials, such as polypyrrole, carbon nanotubes (CNTs), and ferrocene, have been successfully incorporated for this purpose. Generally, relatively weak electric pulses (~1 V) are applied to induce structural changes [70–72]. Thermo-responsive polymers experience a phase transition above or below a particular temperature, referred to as the upper critical solution temperature (UCST) or the lower critical solution temperature (LCST), respectively. UCST is a critical temperature above which the thermo-responsive polymers are soluble and, below which, are insoluble. By contrast, LCST is a critical temperature below which the thermo-responsive polymers are soluble, and, above, which, are insoluble. These values are polymer specific and used to design thermos-responsive structures according to the intended application, as well as the site of action. Poly(*N*-isopropyl acrylamide) (PNIPAAm) is a well-known thermo-responsive polymer with an LCST of ~32 °C; it becomes hydrophobic at this temperature. It is necessary to either modify its side chains, polymeric architecture, or molecular weight, or copolymerize it with the other polymers to tailor the transition temperature suitable for biomedical applications [73–76].

Ultrasound

Three crucial steps should be followed to improve the efficiency of the current CTP and develop an optimized approach (Fig. 3): (i)

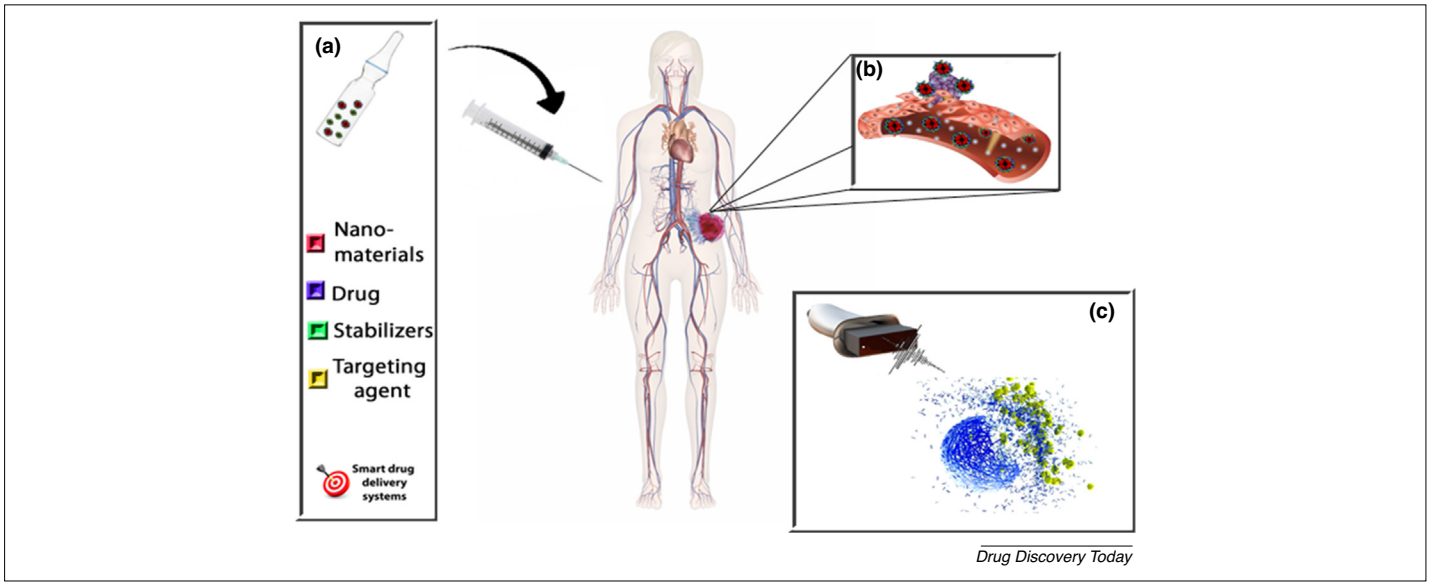

FIGURE 3

Engineering approach to drug delivery systems design. **(a)** Formulating the appropriate nanocarrier, **(b)** accumulation of the nanocarrier in the target site through passive and active targeting, and **(c)** applying ultrasound to trigger drug release from the nanocarrier.

encapsulation of drug into carriers; (ii) targeting drug carriers to the desired location; and (iii) employing triggering mechanisms to release the drug from its carrier.

US refers to mechanical waves with frequencies of 20 kHz to 30 MHz that are used for diagnosis and therapy [77,78]. Table 2 presents examples of applications of US at various frequency ranges. US waves are non-ionizing and, thus, constitute a form of non-invasive radiation that transfers energy onto biological tissues with a relatively low risk of adverse effects. US waves have also been applied as a strategy for US-triggered mechanisms in drug delivery using carrier systems, such as micelles, liposomes, and microbubbles (MBs). The different mechanisms of interaction between the drug carrier system and US promote the uptake and selectiveness in delivering therapeutic agents to the target [79–84]. The significance of US in CTP and its role in triggering drug release from carriers has been known since the late 1990s. As US energy propagates through tissues, it results in heat production, changes in pressure, and mechanical disturbance (non-inertial and inertial cavitation). These mechanisms are generally classified as thermal and nonthermal and could be used for the triggered release of drugs [85–87].

Thermal effects of US waves

Thermal effects arise because of the absorption of acoustic energy by the environment. This could be beneficial in drug delivery by enhancing the diffusion phenomena by cells and could also

TABLE 2

Clinical applications of US

Application	Frequency	Description	Refs
Filtration	28 kHz to 1 MH	As a cleaning mechanism and filtration intensifier through shock waves	[158]
Dentistry	30–150 kHz	Introduces shock waves to fracture calculus, thereby facilitating its removal; provides real-time information about pocket depth, tissue thickness, bone morphology, attachment level, histological change, etc.	[159,160]
Emulsification	>100 kHz	Induces hydrodynamic shear forces to increase effect of emulsification	[161]
Lithotripsy	0.1–1 MHz	Provides shock waves to break up stones in kidney, bladder, or ureter	[162]
Tissue ablation	0.5–1.5 MHz	Provides local heat beyond tolerance of abnormal cells to diminish them	[163]
Drying	>20 kHz	Accelerates mass transfer and increases diffusion to reduce drying time and energy consumption	[164,165]
Sterilization	>20 kHz	Killing pathogens by disrupting cell membrane, producing free radicals and local heat	[166]
Physiotherapy	0.7–3 MHz	Induces local and focused heat within a specific part of body to accelerate healing process via various mechanisms, such as increasing local blood flow	[167]
Defrosting	>20 kHz	Transfers energy to frozen products and reduces thawing time	[168]
Medical imaging	1–20 MHz	Lower frequencies provide images from deeper organs, such as kidney and liver; higher frequency is applied to assess external organs, such as muscles	[169]

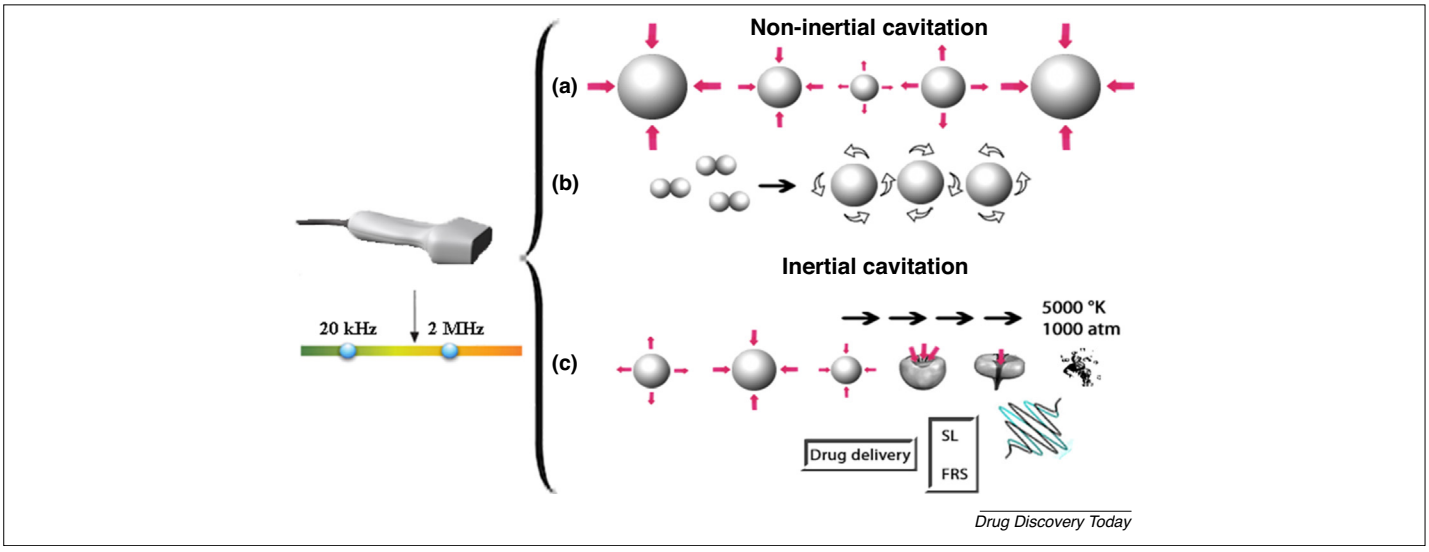

FIGURE 4

Nonthermal effects of ultrasound: **(a)** ultrasonic cavitation, **(b)** non-inertial cavitation, and **(c)** inertial cavitation. Abbreviations: FRS, free radical scavengers; SL, sonoluminescence.

produce a significant response in the pores of the carrier to achieve an accelerated diffusion from the drug delivery system. Moreover, along with the sonoporation effect, which increases the permeability of cancer cells and the carriers, the generated heat following US irradiation can be useful as an adjuvant treatment for patients receiving CTP, because it would render the cancer cells more susceptible to anticancer agents [86,88,89].

Nonthermal effects of US waves

The physical impact of the interaction between US waves (in the 20 kHz to 1 MHz frequency range) and the medium induces molecule displacement or vibration, generating high pressure (compression) when particles are pushed together and low pressure (rarefaction) zones when particles are drawn apart [90,91]. The extent and type of vibration of the molecules induced by the US energy applied to depend on the compressibility, elasticity, and density of the material [92]. In gas-filled cavities, such as bubbles in a liquid medium, US waves induce the formation, volumetric expansion, and contraction of bubbles in response to pressure changes caused by the acoustic field; a process known as acoustic cavitation (Fig. 4). Depending on the oscillating behavior of bubbles, cavitation can be either non-inertial or inertial [93,94].

Non-inertial cavitation

This kind of cavitation occurs when bubbles oscillate within a stable resonance diameter, without collapsing, over many acoustic cycles at a low-intensity acoustic field (Fig. 4a) [92,93,95–97]. When bubbles are exposed to the US rarefaction phase, they can grow through either rectified diffusion or coalescence. In the former case, dissolved gases in the environment accumulate into the bubbles and cause them to grow. Coalescence occurs when several bubbles combine to form a much larger bubble. In this case, the bubble motion creates a circulating fluid flow or local swirling around the bubbles (called microstreaming), which facilitates the transport of therapeutic molecules at high velocities within blood through convection (Fig. 4b). This process can induce reversible cell deformation and membrane permeabilization of deep targets in response to low acoustic pressures [93,94,97–99]. The increased oscillating amplitude of the bubbles, derived from microstreaming, is capable of producing enough shear forces to destabilize the carriers and promote the drug release.

Inertial cavitation

Inertial cavitation occurs when a high-intensity acoustic field is applied, whereby bubbles respond nonlinearly to the driving force, causing them to rapidly increase in size until the expansion exceeds the resonant bubble diameter during the rarefaction phase. As a result, during the compression phase over short acoustic cycles, the bubbles collapse violently, with the velocity approaching the speed of sound [91,93,100]. These mechanical effects generate incredibly high temperatures (5000 K) and pressures (1000 atm) in nanometric boundaries, which, in turn, lead to the production of shockwaves with an initial velocity of 1000 m/s. The accompanying high-speed liquid microjets (when cavitation occurs near a solid surface), emission of light (known as sonoluminescence: SL), and free radical scavengers can be used in the release of drugs from carrier system (Fig. 4c) [92,94,96,97,101,102].

The intensity of the mechanical damage produced by microjets and shockwaves depends on the impact parameters, such as the distance between the cavitating bubble and rigid structures [94,103,104], which can induce cell membrane fragmentation and extravasation without killing the cells and can even generate hydrolysis and free radicals. These phenomena can produce enough energy to break carrier systems and improve the release and transport of drugs into the target cell [105–108].

US-responsive lipid-based drug delivery systems

Drug delivery efficiency is governed by the carrier system response to the US waves and the acoustic parameters used, such as

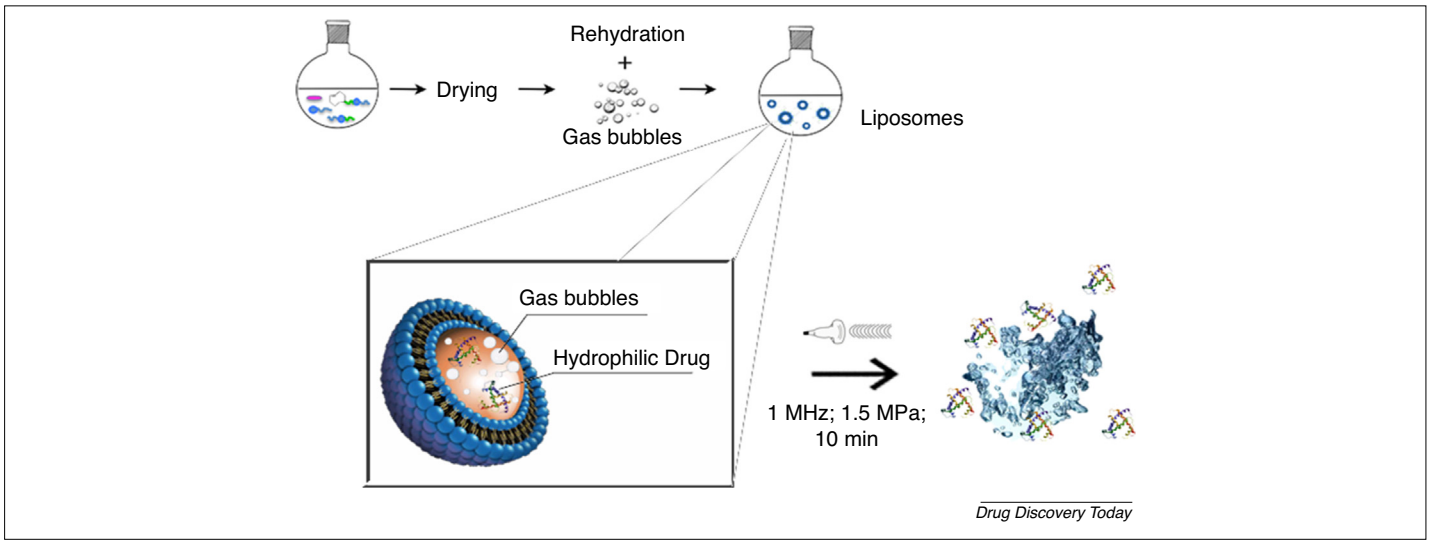

FIGURE 5

Schematic of echogenic liposomes used for drug delivery. When ultrasound exposes such a liposome, it is warmed, becomes permeable, and releases its cargo. This is attributed to cavitation phenomena if low-frequency ultrasound is used and thermal phenomena for high-frequency ultrasound.

frequency (kHz or MHz), pressure (MPa) or intensity levels (W/cm^2), US duty factor (percentage or fraction of time that the system transmits US waves) and exposure duration. Here, we discuss the application of US in combination with some widely used lipid-based drug carriers as a potential means of achieving a targeted CTP strategy.

Liposomes

Liposomes comprise an aqueous core enclosed by one or more lipid bilayers. The liposome membrane typically comprises phospholipids with polar hydrophilic heads and nonpolar lipophilic tails [109–111]. Hydrophilic drugs are encapsulated in the aqueous core, whereas lipophilic drugs are dissolved in the hydrophilic membrane [112]. This carrier is classified in terms of the size and number of lipid bilayers. Given that the liposome diameter ranges from 25 nm to 25 mm [86], liposomes with one aqueous compartment are denoted as unilamellar vesicles (50 – 250 nm), whereas those comprising more than one aqueous chamber are known as multilamellar vesicles (100–1000 nm) [7,113]. Premature drug release from liposomes during storage, as well as in blood circulation, is their main drawback. Most of the phospholipids used for liposome formulation have a phase transition temperature of around the physiological temperature (37 °C), which results in the phase transition of constituent phospholipids and drug leakage. It is proposed that manipulation of the lipid bilayer composition and utilizing phospholipids with higher phase transition temperatures would stabilize the liposome structure [114]. Moreover, the addition of cholesterol stabilizes the liposomal vesicles in physiological media [115].

Several studies have reported the use of US as a trigger for drug release from liposomes [113,116–119]. One strategy to sensitize liposomes to US is to design vesicles containing a gaseous or emulsion phase, which is called an echogenic liposome. Lattin *et al.* reported liposomes containing various liquid emulsions (eLiposomes), such as perfluorocarbon (PFC), which can be activated by US. Following US irradiation, the local pressure of the medium is diminished below the liquid emulsion pressure and causes the PFC to boil and convert to the gaseous phase [110,116]. Another type of liposome that can respond to US is a TSL. When US exposes a TSL, it warms and is converted from a solid-order phase to a liquid-disorder phase and vice versa. Under such a phase transition, liposomes become permeable and release their cargo. Generally, drug release from a TSL can be attributed to cavitation phenomena if low-frequency US is used and thermal phenomena for high-frequency US [120–122]. Liposome-tested nanobubbles, CO_2 gas-generated liposomes, bubble liposomes, and liposome-loaded MBs are other types of echogenic liposomes utilized for drug delivery [123–126] (Fig. 5).

In vitro experiments related to liposomes

Table 3 summarizes recent *in vitro* studies using US to augment drug release from the liposome. Novell *et al.* investigated the effect of focused US (1 MHz; 1.5 MPa; 10 min) on calcein release from TSLs and non-TSLs (NTSLs). For this purpose, 25 ml of calcein-loaded liposomes were diluted in 500 ml of phosphate buffer saline (PBS) and placed into a sample holder. Following US irradiation, the rate of drug release from TSLs increased by ~44% because of the increase in temperature from 37 °C to 42 °C. By contrast, no substantial drug release was observed from NTSLs under the US exposure. Additional calcein release up to 12% was also found by increasing the negative pressure of US from 1.5 MPa to 2 MPa for both TSLs and NTSLs. This rate was related to the mechanical effects of US, such as collapse-inertial cavitation and microstreaming [127]. In addition, Lin *et al.* [128] evaluated the impact of low-frequency US (20 kHz; 1 W/cm^2; 2 s) on DOX uptake by HeLa cells from emulsion liposome (eLipoDOX). They measured the number of viable cells by hemocytometer counting. Their results demonstrated that cell viability was diminished from 100% for untreated cells to 90%, 40%, 60%, and 20% for US only,

TABLE 3

Summary of *in vitro* studies on the combined effect of drug-encapsulated liposomes and US[a]

Nanoparticle	Medium	Targeting moiety	Drug	US parameters	Cell line	Significant results	Refs
eLipoDOX	HeLa cells; cervix	NA	DOX	0.02 MHz, 1 W/cm^2, 0.33 min, CW	HeLa cells	80% cancer cell lethality	[128]
iRGD-PTX-LMC	PBS	iRGD	PTX	1 MHz, 0, 10, 30 or 60 s pulse	bEnd.3 cells and 4T1 cells	Release of ~84.77% of entrapped PTX after 60 s irradiation; significant cell lethality	[170]
Liposome	PBS	NA	FITC	1.1 MHz, 900 W/cm^2, 10 s, 20 s, 30 s, 40 s, 50 s, and 60 s, CW	NA	~21.2% drug release after 10 s exposure; ~70.2% drug release after 10 s exposure	[129]
Liposome-loaded (lipid-shelled) MBs	PBS	NA	DOX	1 MHz, 2 W/cm^2	BLM cells	US-triggered drug release; killing of melanoma cells even at low doses of DOX	[171]
LMB	SDS/Ethanol	Folate	Curcumin	0.7 MHz	MCF 7 cells	Significant accumulation in cells	[172]
	Tween water solution	Folate	Oridonin	1 MHz, 0.5 W/cm^2; 60 s	HepG-2 cells	94% drug release, IC_{50} of 0.508 $\pm$ 0.018 μmol/ml	[173]
MB–liposome pendant structure	PBS	NA	Calcein, thrombin	1 MHz	Canine blood	~30% release of entrapped calcein; ~11% release of entrapped thrombin	[174]
NB-PTXLp	PBS/methanol (70:30 v/v)	NA	PTX	1 MHz, 1 W/cm^2, 75% duty cycle, 30 s	MiaPaCa-2, Panc-1, MDA-MB-231, and AW-8507 cell lines	2.5-fold higher uptake compared with control, 300-fold higher anticancer activity of NB-PTXLps compared with control	[175]
PC:DPPE-PEG	HEPES buffer	NA	Calcein	20 kHz, 2 W/cm^2	NA	Poly- and oligo (ethylene oxide) additives facilitate drug release to reduce energy required	[176]
PEG-liposome	HEPES buffer	NA	Calcein	20 kHz, 2 W/cm^2	NA	Underlying defect-mediated permeabilization mechanism	[177]
PEGylated liposome	*In vitro* skin absorption test using Franz diffusion cells	NA	Fluorescein	20 kHz, 2 min, CW	NA	50% increase in skin permeation profile	[147]
SL	PBS	NA	VIN	1 MHz, 1.5 W/cm^2, 110 s	MCF-7 cells	Burst release (~90%) of VIN	[179]
SSL	PBS	NA	DOX, MPS, cisplatin	20 kHz, 0 to 7 W/cm^2, 0–3 min	Cisplatin-sensitive C26 murine colon adenocarcinoma cells	~80% drug release, US irradiation time-dependent toxicity	[118]
TSLs, NTSLs	NA	NA	DOX	0.8 MHz, 1–3 W/cm^2, 30–120 s	HeLa cells	2.5–5 times lower IC_{50} than free DOX, nucleus internalization of DOX-TSLs, cytoplasm internalization of DOX-NTSLs	[180]

TABLE 3 (*Continued*)

Nanoparticle	Medium	Targeting moiety	Drug	US parameters	Cell line	Significant results	Refs
TSLs, NTSLs	PBS	NA	Calcein	1 MHz, 10 min, pulse	NA	>50% drug release (42 °C)	[127]
USL	NA	NA	ML1	1.3 MHz, 2–24 MPa	CT26	80% drug release, IC_{50} of 400 ng/ml	[178]

[a] Abbreviations: 2-dipalmitoyl-sn-glycerol-3-phosphoethanolamine-N-methoxy; BLM cells, melanoma cells. CW, continuous wave; DPPE, 1; eLipoDOX, emulsion liposome doxorubicin; HEPES, 4-(2-hydroxyethyl)-1-piperazineethanesulfonic acid); HMME, sonosensitive liposomes; iRGD-PTX-LMC, iRGD-targeted paclitaxel-loaded liposome-MB complexes; LMB, Liposome MBs; ML1, Mistletoe lectin-1; MPS, methylprednisolone hemisuccinate; NA, not applicable; NB-PTXLp, nanobubble-paclitaxel liposome; nSSL, nonsterically stabilized liposomes; PBS, phosphate buffer saline; PC, phosphatidylcholine; PEG, poly (ethylene glycol); PTX, paclitaxel; SDS, sodium dodecyl sulfate; SL, sterically stabilized liposome; USL, US-sensitive liposomes; VIN, vincristine bitartrate.

free DOX, eLipoDOX, and eLipoDOX + US treatment groups, respectively. Therefore, the use of US can enhance the rate of drug release from liposomes to achieve a better therapeutic result, while preserving healthy tissue from the adverse effects caused by free drug administration. A feasibility study for applications of high-intensity focused US (HIFU) at a MHz frequency to induce controlled release of the drug content was also carried out. Using dynamic light scattering and transmission electron microscopic observations, Chen *et al.* demonstrated 21.2% of encapsulated fluorescent materials (FITC) were released from liposomes with an average diameter of 210 nm when exposed to continuous (cw) US at 1.1 MHz (I_{SPTA} = 900 W/cm^2) for 10 s and the percentage release efficiency was 70% after 60 s irradiation. This result also reveals that rupture of relatively large liposomes (>100 nm) and generation of pore-like defects in the membrane of small liposomes (<100 nm) because of HIFU excitation might be the main causes of the release; in addition, inertial cavitation occurred during the irradiation. Thus, the controlled drug release from liposomes by HIFU is a potentially useful modality for clinical applications [129].

Zhang *et al.* [130] fabricated dual-responsive nanotheranostics based on gold nanorods (GNRs) bearing liposomes. They incorporated the fabricated GNRs into liposomes synthesized from 1,2-distearoyl-sn-glycero-3-phosphoethanolamine-*N*-[methoxy(polyethylene glycol)-2000]-folic acid (DSPE-PEG2000-FA) liposomes (Fig. 6). The characterization showed that the synthesized GNRs were effectively encapsulated in liposomes, and the resulted constructs were near-infrared (NIR) light (808 nm, 1.6 W/cm^2) and US (1 Hz and 1 W) responsive as a function of temperature elevation. The authors reported that ~30% of the encapsulated drug was released from the carrier over 24 h at physiological temperatures (37 °C), whereas almost 85% drug release was obtained under hyperthermic temperatures (42 °C). Cell toxicity assessments against MCF-7 cells showed that US stimulation of FA-GNR-ABC-DOX/lips resulted in the highest cell toxicity effect. *In vivo* studies on S180 tumor-bearing mice showed that the combinatorial therapy (formulation with stimulation) reduced the weight and relative tumor volume, indicating the tumor inhibition efficiency of the treatments. The tumor imaging capability of the formulated liposomes was investigated via both US imaging and X-ray CT imaging *in vivo*. The results illustrated that the synthesized liposomes exhibited high echo and a functional imaging effect after 30 min post i.v. injection with clear contrast-enhanced signals, which lasted up to 240 min. Moreover, X-ray CT imaging revealed that the formulation provided a CT value of ~920 HU, which was approximately threefold more than the positive control (injected iodine). These data indicate the multimodal theranostic capability of the formulated liposomes for tumor imaging and therapy.

In vivo experiments related to liposomes

Table 4 summarizes recent *in vivo* studies using US to augment drug release from liposomes. Staruch *et al.* investigated the effect of TSL doxorubicin (TLD) on rabbits with VX2 tight tumors in the presence and absence of mild hyperthermia induced by a magnetic resonance-guided HIFU (MR-HIFU) device (1.2 MHz, 42 °C) The tumor growth rate was substantially inhibited with a single infusion of TLD and concurrent hyperthermia induced by HIFU compared with tumors treated with TLD alone within 24 days

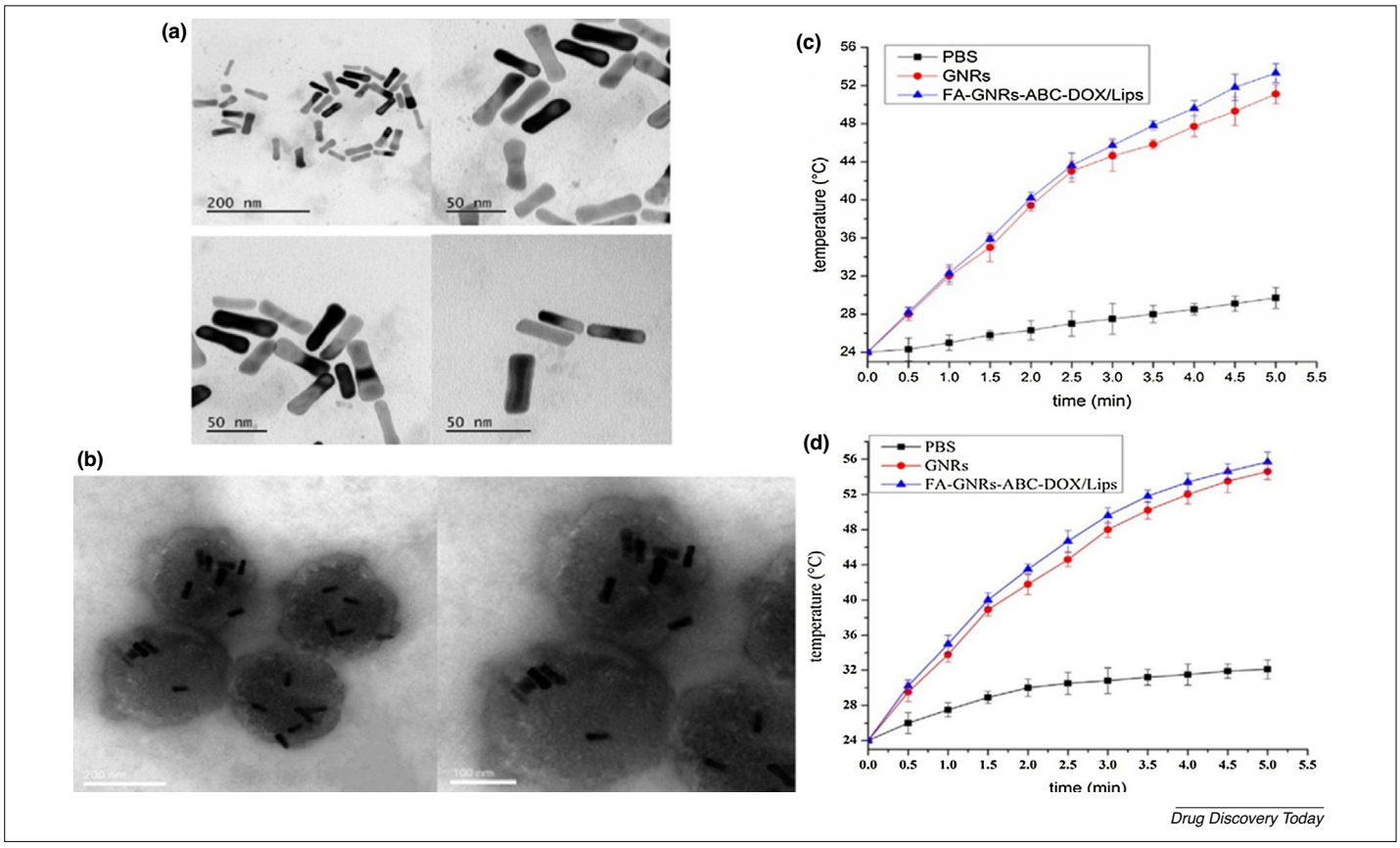

FIGURE 6

TEM micrographs of gold nanorods (GNRs) **(a)** and folic acid (FA)-GNR-Ammonium bicarbonate (ABC)-doxorubicin (DOX)/liposomes **(b)**. Thermal behavior of phosphate buffer saline (PBS), GNRs, and FA-GNR-ABC-DOX/liposomes under stimulation with near-infrared (NIR) light (808 nm, 1.6 W/cm^2) **(c)** and US (1 Hz and 1 W) **(d)**. Reproduced, with permission, from [142].

of treatment. Furthermore, all of the rabbits receiving TLD alone perished over the following 21 days, whereas 70% of rabbits subjected to TLD plus HIFU survived for over 60 days [131]. In another study, Lin *et al.* studied the combined effect of DOX-loaded cationic liposomes (CLs) and focused US (FUS) on the survival rate of rats bearing intracranial C6 glioma tumors. The equivalent dose of DOX was 5.67 mg/kg, which was intravenously administered twice a week. Survival rates of 30.4, 35, and 81.2 days were recorded for animals treated with free DOX, DOX-CLs, and DOX-CLs + FUS, respectively. However, the encapsulation of DOX into CLs did not significantly improve the survival rate. The stimulation of this nanovehicle by focused US dramatically enhanced the efficacy of the CTP regime by prolonging the animal survival rate. Evjen *et al.* [132] assessed the effect of liposome composition on the release behavior of encapsulated payload under US stimulation. They fabricated dioleoyl phosphatidyl ethanolamine (DOPE)-based liposomes and hydrogenated soy phosphatidylcholine (HSPC)-based liposomes. They used near-infrared fluorochrome Al (III) phthalocyanine chloride tetrasulfonic acid ($AlPcS_4$) as the drug model. They reported that AlPcS4 was effectively encapsulated in both liposomes, confirmed by the concentration-dependent quenching of fluorescence. *In vitro* stability and release studies showed that the liposomes were stable in serum samples without any fluorescence signal. US stimulation (1.1 MHz with the corresponding ISPPA of 10.5 kW/cm^2) showed that the DOPE-based liposomes (~40% drug release after 1 min) were more sonosensitive than were HSPC-based liposomes (~20% drug release after 1 min). *In vivo* studies (Fig. 7) revealed that US stimulation significantly triggered the release of $AlPcS_4$ from DOPE-based liposomes and resulted in a 100% increase in fluorescence signal intensity ($P < 0.05$), where no signal enhancement was observed with HSPC-based liposomes after US stimulation. Moreover, the signal intensity of the control group (liposomes without stimulation) did not change during the study, indicating the US-dependent release of $AlPcS_4$.

Microbubbles

Devices based on MBs are another type of US responsive nonvehicle and comprise a gaseous core and a shell that is composed of phospholipids, proteins, or polymers (Fig. 8). Given their large size (1–10 mm), MBs cannot passively extravagate in solid tumors [97,133]. When MBs are exposed to US, they volumetrically oscillate owing to the compressible nature of their gas core. Also, MBs can act as cavitation nuclei in the acoustic field, producing shear force, acoustic streaming, inertia, and stable cavitation [134–136]. All these effects could facilitate drug release from MBs, as well as enhance the permeability of the cell membranes.

Based on coating type, MBs are divided into two categories; soft-shelled and hard-shelled MBs. Soft-shelled MBs are fabricated from thin surfactants, such as phospholipid or protein, which makes

TABLE 4

Summary of *in vivo* studies conducted on combined effects of drug-encapsulated liposomes and US[a]

Nanoparticle type	Tumor; origin	Drug	Route	US parameters	Animal model	Significant results	Refs
iRGD-PTX-LMC	4T1 cells; breast	PTX	IV	1 MHz, 0, 10, 30 or 60 s, pulse	Female BALB/c mice	Significant tumor inhibition	[170]
SL	MCF-7; breast	VIN	IV	1 MHz, 1.5 W/cm^2, 110 s	Female BALB/c mice	Significant tumor inhibition, longest median survival time, 40 days	[179]
LMB	HepG-2 cells; liver	Oridonin		1 MHz, 0.5 W/cm^2, 60 s	BALB/c nude mice	Tumor inhibition ratio 87.6%	[173]
DOX-CLs	C6 glioma; brain	DOX	IV	1 MHz, 0.32 W, 1 min	C6 glioma rats	~83.47% tumor inhibition	[181]
Doxo-Gado-Lipo	TS/A; breast	DOX	IV	3 MHz, 5.4 W/cm^2, 2 min, pulsed	Mice bearing mammary adenocarcinoma	~100% tumor inhibition	[182]
LCLP-Dox	CT26; colon	DOX	IV	1.5 MHz, 83.35 W/cm^2, 2 min, pulsed	Mice bearing CT26 solid tumors	~42.11% tumor inhibition	[183]
TLD	Vx2; pyriform sinus	DOX	IV	1.2 MHz, CW	Rabbits bearing Vx2 tumors	~100% tumor inhibition	[131]
CuDox-LTSLs	NDL; breast	DOX	IV	1.54 MHz, pulsed	Mice bearing 46 NDL tumors	~100% tumor inhibition	[184]
nSSL	J6456 murine lymphoma tumors	Cisplatin	i.p.	20-kHz, 5.9 W/cm^2, 2 min, CW	Mice bearing J6456 murine lymphoma	~70% drug release in tumor site; tumors stopped proliferating and then regressed over time	[102]
LTSL	Murine mammary adenocarcinoma	DOX	IV	1 Hz, 1,300 W/cm^2, 15–20 min, pulsed	Mice bearing mammary adenocarcinoma	~50% drug release after 2 min exposure; US reduced tumor size and growth	[185]
Caelyx	WiDr; human colon cancer	DOX	IV	20 kHz, 3.16 W cm^2, 30 min, CW	Mice bearing human colon carcinoma	US + DOX significantly reduced tumor size	[186]
Long-circulating pegylated liposomes	9L rat glioma tumors	DOX	IV	1 Hz, 60 s	L9 glioma rats	100% increase in median survival	[60]
Liposomal doxorubicin	9L rat gliosarcoma tumors	DOX	IV	1.7 MHz	L9 glioma rats	24% increase in median survival	[187]
Liposomal doxorubicin	SCC7; murine squamous cell carcinoma cell line	DOX	IV	1.5 MHz, 1114 W/cm^2, 5 min	Mice bearing squamous cell carcinoma	124% higher drug concentration in tumor	[188]
MB-Lipo	VX2 tumor; squamous cell carcinoma	DOX	IA	5–12 MHz, 1 min	Rabbits bearing Vx2 tumors	Significant tumor size-reduction; targeted drug accumulation in tumor site	[189]
PLMC	4T1-tumor; breast	PTX	IV	1 MHz, 5 s, 10 s, 30 s, or 60 s	Mice bearing 4T1 tumors	74.39% angiogenesis reduction in tumor xenografts; significant tumor size reduction	[119]
PEG-liposome	DHD/K12 tumors; colon	DOX	IV	20-kHz, 1 W/cm^2, 15 min	Rats bearing DHD/K12 tumors	Significant tumor size-reduction	[190]
DOPE-based and HSPC-based liposomes	22Rv1, human prostate	AlPcS4	IV	1.1 MHz, (ISPPA) 10.5, kW/cm^2, 10 to 60 s	Mice bearing 22Rv1 human prostate tumors	DOPE-based liposomes showed superior song sensitivity compared with HSPC-based liposomes	[132]

[a] Abbreviations: AlPcS4, Al (III) phthalocyanine chloride tetrasufonic acid; Caelyx, liposomally encapsulated DOX; CuDox-LTSLs, Copper-DOX lysolipid-containing temperature-sensitive liposomes; DOX-CLs, DOX-loaded cationic liposomes; Doxo-Gado-Lipo, DOX-Gadoteridol liposome; HMME, sonosensitive liposomes; IA, intra-arterial administration; iRGD-PTX-LMC, iRGD-targeted paclitaxel-loaded liposome-MB complexes; LCLP-Dox, PEGylated liposomal DOX; MB-Lipo, MB-liposome complex; nSSL, nanosterically stabilized liposomes; PLMC, PTX-liposome-MB complexes; PTX, paclitaxel; VIN, vincristine bitartrate.

them highly sensitive to US. In this type of MB, the drug loading rate is very low. To improve this, a drug can also be loaded onto the surface of the shell. The latter refers to MBs that are coated with a polymer with the benefits of higher stability and higher drug loading rate versus soft-shelled MBs. However, the polymeric coating diminishes the sensitivity of MBs to US [97]. Recently, researchers conducted studies on nanocarrier-MB hybrids, which were fabricated by attaching various drug carriers, such as

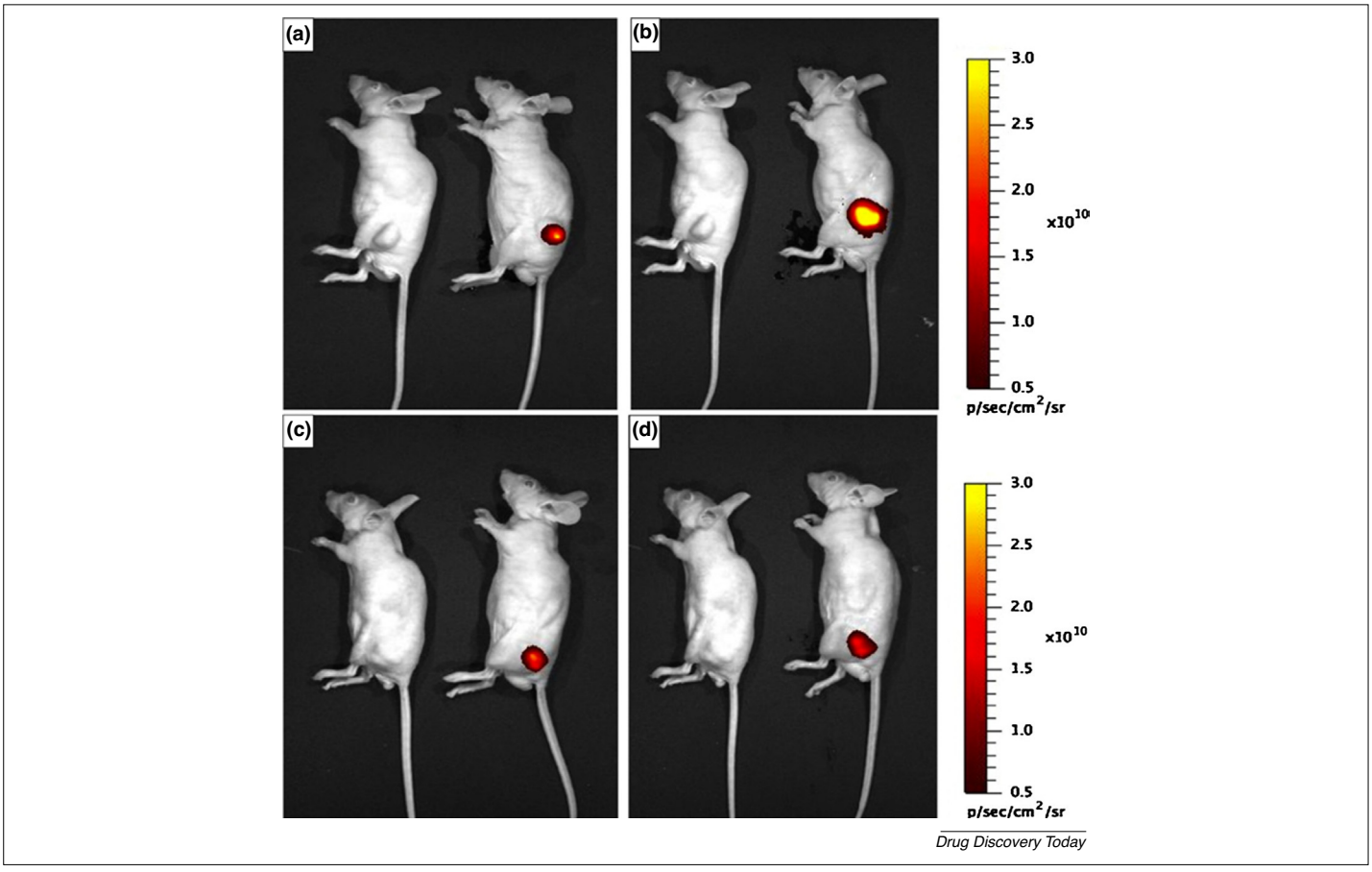

FIGURE 7

In vivo studies of US stimulation triggered the release of AlPcS4 from DOPE-based liposomes. Mice were administered with $AlPcS_4$-containing DOPE-based **(a,b)** and $AlPcS_4$-containing HSPC-based liposomes **(c,d)**, before (a,c) and after (b,d) ultrasound (US) stimulation. The animals on the left in the images are the controls. Reproduced, with permission, from [132].

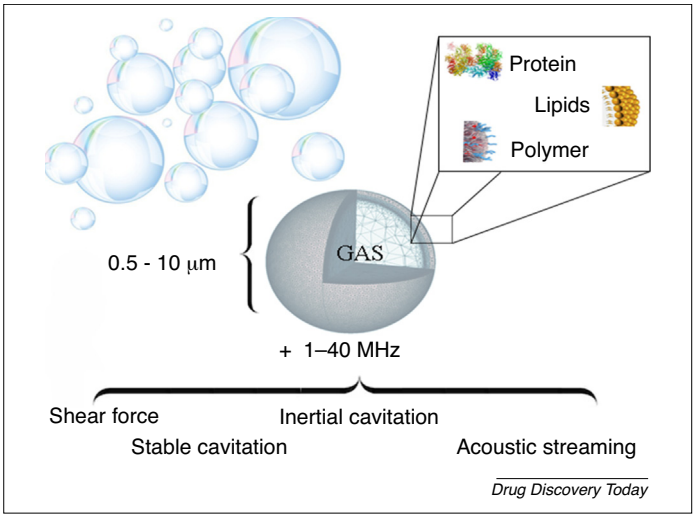

FIGURE 8

A typical device for microbubble (MB) delivery. The image shows different shell compositions, (lipids, polymers, and proteins) and beneficial ultrasound-mediated effects of microbubbles (shear force, internal cavitation, stable cavitation, and acoustic streaming).

liposomes, micelles, or other NPs, to the surface of the MBs [137] (Fig. 9). Such hybrid platforms bring the advantages of high drug loading capacity, target specificity, and vascular permeabilizing effect of MBs. Furthermore, this unique configuration could have diagnostic abilities. For example, Fan *et al.* presented DOX-loaded MBs containing superparamagnetic iron oxide (SPIO) as CTP and magnetic resonance imaging (MRI) contrast agents [138].

In vitro studies related to MBs

Table 5 summarizes recent *in vitro* studies using US to augment drug release from MBs. Hu *et al.* synthesized a unique MB-based hybrid carrier structure for targeted delivery of sunitinib in the presence of US exposure (1 MHz, 2.2 W/cm^2) and studied its therapeutic effects on GRC-1 renal carcinoma cells. Liposomes containing sunitinib were prepared and then adsorbed to the surface of MBs to form sunitinib-loaded MBs. The combined action of sunitinib-loaded MBs and US led to a remarkable reduction in cell survival and showed better therapeutic benefits versus the free sunitinib treatment group, including lower cell survival and higher apoptosis rate [139]. Sun *et al.* synthesized oxygen and PTX-loaded lipid MBs (OPLMBs) for US-mediated CTP against hypoxic ovarian cancer cells. They successfully demonstrated that

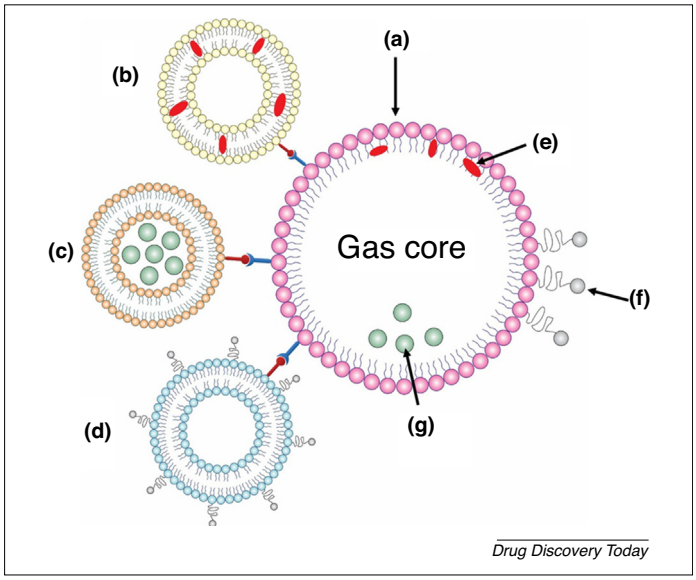

FIGURE 9

Drug and liposome-loaded microbubbles (MBs). **(a)** Lipid-based MB, **(b)** hydrophobic drug-encapsulated liposome, **(c)** hydrophilic drug encapsulated within the aqueous core of the liposome, **(d)** liposome with surface drug conjugated, **(e)** hydrophobic drug entrapped within phospholipid membrane of MB, **(f)** drug conjugated onto the surface of phospholipids, and **(g)** drug encapsulated microbubble.

US-induced OPLMBs destruction significantly enhanced local oxygen release to mitigate hypoxia and intensify the cytotoxic effect of the anticancer drug. They also indicated that OPLMBs, in combination with US (300 kHz, 0.5 W/cm^2, 15 s) yielded a superior antiproliferative activity of 52.8% and a cell apoptosis ratio of 35.25% in hypoxic cells relative to another treatment group at 24 h after treatment. This experiment suggested US mediation of oxygen and drug-loaded MBs as a useful method to overcome chemoresistance in hypoxic cancer cells [140].

In vivo studies related to MBs

Table 6 summarizes recent *in vivo* studies using US to augment drug release from MBs. Fan *et al.* presented a new theranostic complex of superparamagnetic iron oxides (SPIO)-DOX- conjugated MBs (SD-MBs) for image-guided drug delivery to the brain. The magnetic component provided enhanced accumulation of the drug within target through magnetic targeting as well as real-time monitoring of the complex under MRI. The authors demonstrated that FUS exposure in a rat glioma model facilitated blood–brain barrier (BBB) opening, highlighting the feasibleness of simultaneous magnetic and US targeting. Consequently, deposition of the complex within the tumor was dramatically increased (25.7-fold for DOX and 7.6-fold for SPIO) [141]. In another study, Wang *et al.* presented a folate-conjugated hybrid carrier based on MBs. They investigated its antitumor activities in the presence of US against liver cancer. Oridonin (ORI) as a CTP agent was loaded into a liposome, and the resulting L-ORI was attached to the MB surface to form LMB-ORI. The highest tumor inhibition rate was achieved in animals receiving folate-conjugated LMB-ORI combined with US (>85%). These results show that this targeted liposome MB plus US enhanced the anticancer effects of ORI as a CTP agent as well as reducing its cardiotoxic adverse effects [142].

Other NPs

In addition to the above-mentioned drug carriers responsive to US, other structures have also revealed enhanced drug delivery under US mediation. Several studies have conducted on various solid NPs, such as micelles, quantum dots, magnetic NPs, and polymeric NPs, which can interact with US [142–146]. One way to sensitize these NPs to US is to attach them to MBs or add them to the

TABLE 5

Recent *in vitro* studies using US to augment drug release from MBs[a]

Carrier	Medium	Drug	US parameters	Cell model	Significant results	Refs
DPPC:DPSE-PEG2000	PBS	calcein	1.1 MHz, 1.06 – 6.75 Mpa, 5 s	NA	52.9 ± 10.3% drug release	[191]
UML	NaCl/sodium citrate/HEPES	CA4P	1.3 and 1.7 MHz, 5 and 120 s	EA.hy926 cell line	9.4 ± 0.2% drug release	[192]
DSPC:DSPE-PEG2000	NA	siRNA-NPs and PTX	1.5 MHz, 10 W/cm^2, 30 s	B16F10 cell line	Significant *VEGF* silencing, significant cell toxicity	[165]
NBs	PBS,	DOX	3 MHz, 2 W/cm^2, 60 s	LS-174T	Significant drug release, 15.9 ± 5.39% cell viability	[193]
DPPG-Na, DSPC-MB	PBS	DOC	0.8 Hz, 2.56 W/cm^2	DLD-1 cells	~ 65% tumor cell toxicity	[194]
DSPC:DSPE-PEG2000: DSPE-PEG2000-biotin	NA	DOX	1 MHz, 1.65 W/cm^2	MCF-7 cell line	High cell death and apoptosis because of increased ROS level, DNA damage, and significant reduction of P-glycoprotein expression	[195]
DPPA/DSP-MB	NA	PTX	300 kHz, 0.5 W/cm^2, 30 s	Ovarian cancer A2780/DDP cells	Antiproliferative activities of 75.93 ± 2.81%; cell apoptosis ratio of 32.6 ± 0.79%	[196]
DPPC/DSPE-PEG-PDP/Liposome	OptiMEM-1% FCS	DOX	1.7 MHz	U-87 MG	~ 70% drug release; fourfold decrease in cell viability	[197]

[a] Abbreviations: DPSE-PEG2000, 1,2-distearoyl-sn-glycero-3-phosphoethanolamine-N-[methoxy(polyethylene glycol)-2000]; DLD-1 cells, human colon adenocarcinoma cell line; DOC, docetaxel; DPPA, 1,2-dipalmitoyl-sn-glycero-3-phosphate; DPPC, dipalmitoyl phosphatidyl choline; DPPG-Na, dipalmitoyl phosphatidyl glycerol (sodium salt); DSPC, distearoyl phosphatidyl choline; FCS, fetal calf serum; NA, not applicable; NBs, nanobubbles; PTX, paclitaxel; ROS, reactive oxygen species; sodium salt; U-87 MG, human glioblastoma cells; VEGF, vascular endothelial growth factor.

TABLE 6

Recent *in vivo* studies using US to augment drug release from MBs[a]

Nanoparticle type	Drug	Route	US parameters	Tumor; origin	Significant results	Refs
DPPA/DSP-MB	PTX	IP	300 KHz, 2 W/cm^2, 3 min	A2780/DDP; ovarian cancer	Increased tumor apoptosis and reduced angiogenesis; increased median survival by 52%	[198]
DPPC, DPPA, DPPE-PEG2000- MD	10-HCPT	IV	1 MHz, 2 W/cm^2, 6 min	H22; murine hepatic cells	Remarkable drug accumulation in tumor tissues; ~70.6% tumor inhibition rate	[199]
DPPC/DSPE-PEG2000	BCNU	BI	1 MHz, 1 min	C-6 glioma cells; brain	Controlled tumor progression (915.3–39.6%); median survival of 29–32.5 days	[200]
DSPC:DSPE-PEG2000	PTX	IV	1.5 MHz, 10 W/cm^2, 30 s	SCC-7; squamous carcinoma	Significant therapeutic efficacy on tumor growth inhibition; significant reduction in *VEGF* expression	[156]
Lipid MB	Evans blue	IV	3 MHz, 0.5 W/cm^2, duty cycle: 50% 3 min	NA	Efficient drug delivery to brain	[201]
	DOC	IV	300 KHz, 2 W/cm^2, 100 s	VX2; liver	Tumor inhibition rate of 30.71%; enhanced tumor cell apoptosis	[202]
			1.3 MHz	DSL6A; pancreatic carcinoma	12-fold higher tissue concentration of drug; significantly lower tumor growth	[203]
NBs	DOX	IV	3 MHz, 2 W/cm^2, 60 s	LS-174T; colorectal cancer	Appropriate distribution of Dox in tumor	[193]
SPIO-NPs- DSPC, DSPG and DSPE-PEG2000-MB	DOX	IV	500-kHz	C-6 glioma cells; brain	Reduced cell viability (~20%); active localization of carrier in tumor	[138]
UML	CA4P	IP	1.3 and 1.7 MHz, 5 and 120 s	CT26; colon carcinoma	150-fold improvement compared with chemotherapy alone	[192]

[a] Abbreviations: DPPC, 1,2-dipalmitoyl-sn-glycero-3-phosphatidylcholine; DPPA, 1,2-dipalmitoyl-sn-glycero-3-phosphate; BCNU, 1,3-bis(2-chloroethyl)-1- nitrosourea; BI, bolus injection; CA4P, combretastatin A4 phosphate; DOC, docetaxel; DPPE, dipalmitoyl phosphatidylethanolamine; IP, intraperitoneal; NBs, nanobubbles; PEG, polyethylene glycol; PTX, paclitaxel; UML, ultramagnetic liposomes; VEGF, vascular endothelial growth factor.

medium contained within the MBs. Interaction of US with MBs can generate acoustic cavitation near the carriers and destroy them, resulting in drug release. Recently, the effects of 3 MHz-US irradiation on the therapeutic ratio of PLGA-based magnetic nanocapsules containing fluorouracil (5FU) were reported. Nanocapsules with a magnetic core were selectively targeted toward colon tumors in BALB/c mice by using an external magnetic field. Subsequently, the tumors were exposed to US (0.3 W/cm^2; 10 min) to accelerate the release of 5FU. A tumor volume of 1500 mm^3 in mice treated with 5FU significantly diminished to ~0 mm^3 after the mice received the combination treatment of a magnetic drug coupled with US [147]. Abed *et al.* [3] evaluated the effect of US on the profile of 5FU release from the same magnetic nanocapsules in PBS and found that US significantly accelerated drug release from the nanocapsules in an intensity- and frequency-dependent manner.

US hyperthermia-induced drug delivery

Hyperthermia is an adjuvant therapy for cancer in which the heat originates from external sources (e.g., laser, radiofrequency waves, and US) that exposes malignant tissue to destroy cancer cells directly or to sensitize them to other treatment modalities, such as radiotherapy and CTP. Nonselectivity in tumor heating using current hyperthermia techniques results in undesired thermal damage to surrounding healthy tissue and limits the application of hyperthermia in the clinic. In this regard, NPs have shown potential in the absorption of hyperthermic energy sources, inducing localized heating [148]. Recent studies reported that some NPs have sonosensitizing properties, which enable them to enhance the thermal and mechanical interactions of US with a tissue [149,150]. More recently, it was found that gold NPs (AuNPs), iron oxide NPs, and nano-graphene oxides exhibit such sonosensitizing capabilities. Colon tumors subjected to these NPs showed an increased heating rate during sonication [151,152].

The combination of hyperthermia and CTP results in suprasynergistic effects in cancer therapy. Incorporation of anticancer drugs into nanocarriers that have sonosensitizing effects and subsequent sonication might provide effective thermo-CTP. US not only triggers drug release from the carriers, but also enhances the heat in the presence of such sonosensitizing carriers and intensifies the cytotoxic effect of loaded drugs [153,154]. Wu *et al.* studied the combined effect of FUS hyperthermia and CTP on brain metastasis of breast cancer *in vivo*. Animals were intravenously injected with PEGylated liposome DOX (PLD) and subjected to FUS hyperthermia (500 KHz, 10 min, 0.97 MPa), ~1 min after injection. They demonstrated that short-term FUS hyperthermia significantly increased the deposition of PLD into brain tumors. Tumor growth inhibition for animals subjected to PLD plus FUS hyperthermia was more prominent compard with other treatment groups. These results revealed that hyperthermia-induced by US could increase PLD delivery into brain tumors by increasing the EPR effect [155].

Rezaeian *et al.* [156] developed a computational model to evaluate the efficacy of HIFU hyperthermia-triggered drug release from TSL-DOX via intraperitoneal (IP) injections. They showed enhanced drug penetration depth under HIFU. Although smaller

TABLE 7

Overview of studies conducted on FUS hyperthermia-triggered drug delivery systems[a]

Formulation	HIFU	Animal/Model	Significant results	Refs
Prohance® and DOX-loaded iLTSL	1.44 MHz; acoustic power, 10–15 W, MR-guidance	Wag/Rij rats/rhabdomyosarcoma	14.6-fold increase in concentration of DOX in irradiated group compared with no-HIFU group (median 2.840%ID/g versus 0.194% ID/g); 2.9 times higher DOX concentration than free DOX group (median, 2.840% ID/g versus 0.985% ID/g)	[204]
	MR-HIFU clinical system (fac = 1.2 MHz)	Rabbit/VX2 tumor	MR signal enhancement	[172]
Prohance® and DOX-loaded TTSL	MR-HIFU clinical system with dedicated animal setup (I_{SATA} = 117 W/cm^2,1.4 MHz, cw)	Rat/9 l tumor	MR signal enhancement; significantly higher tumor DOX concentrations than untreated tumor (7.4 versus 1.5 μg/g tissue)	[205]
ThermoDox®	FUS tumor therapeutic system	Human/hepatic primary or secondary (metastatic) tumors	Average increase of 3·7-fold in intratumoral biopsy DOX concentrations	[157]
	Mechanical scanning (2.8 MHz), MRI guidance	Rabbit/muscle	16.8-fold increase in concentration of DOX irradiated tissues compared with untreated tissue	[193]
	MR-HIFU clinical system	Rabbit/VX2 tumor	Significantly higher tumor DOX concentrations (7.6- and 3.4-fold greater compared with free DOX and LTSL, respectively)	[173]
	Mechanical scanning (2.5 MPa, 2.8 MHz), MRI guidance	Rabbit/muscle	Significantly higher concentration of DOX in irradiated tissues than untreated tissue (8.3 versus 0.5 ng/mg)	[156]
	Split focus transducer (TAT 80 W, 1 MHz duty cycle 10%)	Mice/murine squamous cell carcinoma (SCC7)	Significantly higher concentration of DOX in irradiated tissues than untreated tissue (1.7 versus 0.7 μg/g tissue)	[206]
	Pulsed HIFU (I_{SATA} = 1300 W/cm^2, 120 pulses, prf 1 Hz, duty cycle 10%)	Mice/murine mammary adenocarcinoma; BALB/c	Significantly higher concentration of DOX in irradiated tissues than untreated tissue (3.5 versus 1.5 μg/g tissue)	[185]

[a] Abbreviations: iITSl, imageable thermosensitive liposome; Prohance®, gadolinium-based contrast agent; TAT, total acoustic power.

TSLs provide better treatment efficacy, the size of TSLs should be matched with the permeability of the tumor microvascular and TSLs smaller than the vessel wall pore size exhibit reduced efficiency. Recently, results of a Phase I clinical trial, TARDOX, were released [157]. The study assessed the feasibility and safety of enhanced delivery and targeted drug release of DOX from ThermoDox® (thermally sensitive liposomes), triggered by mild hyperthermia induced by FUS in liver tumors. The authors reported an average increase of 3.7 times after applying FUS compared with non-FUS and concluded that the developed system is clinically safe, feasible, and able to promote intratumoral drug delivery. Table 7 summarizes the most relevant data published relating to FUS hyperthermia-triggered drug release from carries.

Concluding remarks and future perspectives

The high prescribed dose of anticancer drugs and their resulting adverse effects on healthy tissues are two of the major drawbacks of conventional CTP. Using smart carriers to sequester anticancer drugs, directing the carriers toward the tumor site, and using a triggered-release mechanism are urgently required to overcome these limiting adverse effects and to develop a targeted CTP strategy. US as a mediator for accelerating drug release from carriers can promote the efficiency of conventional CTP. Here, we highlighted the potential role of US in combination with widely used drug carriers to achieve a targeted CTP strategy. Some drug carriers,such as liposomes and MBs, because of their intrinsic echogenic properties, exhibit enhanced drug delivery following US activation. In addition, US-induced hyperthermia might be a trigger to release the drug from thermosensitive carriers, such as TSL.

However, there are some barriers to the clinical translation of US-triggered drug delivery systems based on lipid-based nanostructures. These include biological relevance, characterization and screening, large-scale production and reproducibility, safety and pharmacological, and regulatory issues. From a biological point of view, various targeting moieties should be assessed to provide cancer-specific spatial drug targeting. Several studies have been dedicated to resolving this issue. Moreover, special attention must be considered regarding the heterogeneity of tumors in humans, patient-specific biology, and their correlation with the applied animal model. Conducting of *in silico* approaches, such as quantitative structure–activity relationship (QSAR) and molecular dynamic simulations, before experimental studies, as well as the selection of appropriate animal models of disease with the most resemblance to human tumors, will facilitate the clinical translation process.

Quality and cost are located at the center of pharmaceutical manufacturing development; hence, formulations that require complicated and/or laborious production procedures have low clinical translation potential. The current challenges facing manufacturing scale-up and reproducibility are scalability complexities, poor quality control, expensive materials and/or manufacturing, low production yield, batch-to-batch variation in reproducibility and storage stability, imperfect purification from the lack of appropriate infrastructure of contaminants/by-products/starting materials, and scarcity of pharmaceutical industry investment and venture funds. However, recent breakthroughs in the facile and high-throughput synthesis of liposomes could result in the large-scale production of these carriers. In conclusion, US can improve the efficiency of conventional CTP by reducing the adverse effects of the latter and resulting in a site-specific delivery strategy. However, there are issues that need to be addressed to take US-triggered lipid-based carriers from the bench to the clinic.

Acknowledgement

Dr. Amirhossein Ahmadi would like to thanks the Pharmaceutical Sciences Research Center, Faculty of Pharmacy, Mazandaran University of Medical Sciences, Sari, Iran for supporting to publish the paper.

References

1 Siegel, R.L. *et al.* (2019) Cancer statistics, 2019. *CA Cancer J. Clin.* 69, 7–34
2 Shakeri-Zadeh, A. *et al.* (2013) Targeted, monitored, and controlled chemotherapy: a multimodal nanotechnology-based approach against cancer. *ISRN Nanotechnol.* 2013, Article ID 629510 https://doi.org/10.1155/2013/629510
3 Abed, Z. *et al.* (2016) Effects of ultrasound irradiation on the release profile of 5-fluorouracil from magnetic polylactic co-glycolic acid nanocapsules. *J. Biomed. Phys. Eng.* 6, 183
4 Arias, J.L. (2008) Novel strategies to improve the anticancer action of 5-fluorouracil by using drug delivery systems. *Molecules* 13, 2340–2369
5 Afadzi, M. *et al.* (2012) Effect of ultrasound parameters on the release of liposomal calcein. *Ultrasound Med. Biol.* 38, 476–486
6 Marin, A. *et al.* (2001) Acoustic activation of drug delivery from polymeric micelles: effect of pulsed ultrasound. *J. Controlled Release* 71, 239–249
7 Ahmed, S.E. *et al.* (2015) The use of ultrasound to release chemotherapeutic drugs from micelles and liposomes. *J. Drug Target.* 23, 16–42
8 Sun, H. *et al.* (2010) Shell-sheddable micelles based on dextran-SS-poly (ε-caprolactone) diblock copolymer for efficient intracellular release of doxorubicin. *Biomacromolecules* 11, 848–854
9 Sawyers, C. (2004) Targeted cancer therapy. *Nature* 432 (7015), 294
10 Chari, R.V. (2007) Targeted cancer therapy: conferring specificity to cytotoxic drugs. *Acc. Chem. Res.* 41, 98–107
11 Shapira, A. *et al.* (2011) Nanomedicine for targeted cancer therapy: towards the overcoming of drug resistance. *Drug Resist. Updat.* 14, 150–163
12 Ahmadi, A. and Arami, S. (2014) Potential applications of nanoshells in biomedical sciences. *J. Drug Target.* 22, 175–190
13 Azadi, Y. *et al.* (2020) Targeting strategies in therapeutic applications of toxoplasmosis: recent advances in liposomal vaccine delivery systems. *Curr. Drug Targets* 21, 541–558
14 Jaimes-Aguirre, L. *et al.* (2016) Polymer-based drug delivery systems, development and pre-clinical status. *Curr. Pharm. Des.* 22 (19), 2886–2903
15 Enrique, M.-A. *et al.* (2015) Multifunctional radiolabeled nanoparticles: strategies and novel classification of radiopharmaceuticals for cancer treatment. *J. Drug Target.* 23, 191–201
16 Mirshojaei, S.F. *et al.* (2016) Radiolabelled nanoparticles: novel classification of radiopharmaceuticals for molecular imaging of cancer. *J. Drug Target.* 24, 91–101
17 Shakeri-Zadeh, A. *et al.* (2014) A scientific paradigm for targeted nanophotothermolysis; the potential for nanosurgery of cancer. *Lasers Med. Sci.* 29, 847–853
18 Peer, D. *et al.* (2007) Nanocarriers as an emerging platform for cancer therapy. *Nat. Nanotechnol.* 2, 751
19 Wang, M.D. *et al.* (2007) Nanotechnology for targeted cancer therapy. *Expert Rev. Anticancer Ther.* 7, 833–837
20 Yingchoncharoen, P. *et al.* (2016) Lipid-based drug delivery systems in cancer therapy: what is available and what is yet to come. *Pharmacol. Rev.* 68, 701–787
21 Miller, A.D. (2013) Lipid-based nanoparticles in cancer diagnosis and therapy. *J. Drug Deliv.* 2013, Article ID 165981 https://doi.org/10.1155/2013/165981
22 Moreira, J. *et al.* (2008) Non-viral lipid-based nanoparticles for targeted cancer systemic gene silencing. *J. Nanosci. Nanotechnol.* 8, 2187–2204
23 Vasir, J.K. and Labhasetwar, V. (2005) Targeted drug delivery in cancer therapy. *Technol. Cancer Res. Treat.* 4, 363–374
24 Mura, S. *et al.* (2013) Stimuli-responsive nanocarriers for drug delivery. *Nat. Mater.* 12, 991
25 Thambi, T. and Lee, D.S. (2019) Stimuli-responsive polymersomes for cancer therapy. In *Stimuli Responsive Polymeric Nanocarriers for Drug Delivery Applications* (Makhlouf, Abdel Salam Hamdy and Abu-Thabit, Nedal Y., eds), Elsevier, Woodhead Publishing Series in Biomaterials
26 Paris, J.L. *et al.* (2017) Vectorization of ultrasound-responsive nanoparticles in placental mesenchymal stem cells for cancer therapy. *Nanoscale* 9 (17), 5528–5537
27 Rapoport, N.Y. *et al.* (2009) Controlled and targeted tumor chemotherapy by ultrasound-activated nanoemulsions/microbubbles. *J. Controlled Release* 138, 268–276
28 Zhou, Y. *et al.* (2013) Microbubbles from gas-generating perfluorohexane nanoemulsions for targeted temperature-sensitive ultrasonography and synergistic HIFU ablation of tumors. *Adv. Mater.* 25 (30), 4123–4130
29 Elkhodiry, M.A. *et al.* (2016) Synergistic nanomedicine: passive, active, and ultrasound-triggered drug delivery in cancer treatment. *J. Nanosci. Nanotechnol.* 16, 1–18
30 Moussa, G.H. *et al.* (2015) Review on triggered liposomal drug delivery with a focus on ultrasound. *Curr. Cancer Drug Targets* 15, 282–313
31 Javadi, M. *et al.* (2013) Ultrasonic gene and drug delivery using eLiposomes. *J. Controlled Release* 167, 92–100
32 Golombek, S.K. *et al.* (2018) Tumor targeting via EPR: strategies to enhance patient responses. *Adv. Drug Deliv. Rev.* 130, 17–38
33 Maeda, H. *et al.* (2013) The EPR effect for macromolecular drug delivery to solid tumors: improvement of tumor uptake, lowering of systemic toxicity, and distinct tumor imaging *in vivo*. *Adv. Drug Deliv. Rev.* 65, 71–79
34 Fang, J. *et al.* (2011) The EPR effect: unique features of tumor blood vessels for drug delivery, factors involved, and limitations and augmentation of the effect. *Adv. Drug Deliv. Rev.* 63, 136–151
35 Allen, T.M. (2002) Ligand-targeted therapeutics in anticancer therapy. *Nat. Rev. Cancer* 2, 750–763
36 Bertrand, N. *et al.* (2014) Cancer nanotechnology: the impact of passive and active targeting in the era of modern cancer biology. *Adv. Drug Deliv. Rev.* 66, 2–25
37 Danhier, F. *et al.* (2010) To exploit the tumor microenvironment: passive and active tumor targeting of nanocarriers for anti-cancer drug delivery. *J. Controlled Release* 148, 135–146
38 Gujral, S. and Khatri, S. (2013) A review on basic concept of drug targeting and drug carrier system. *IJAPBC* 2, 2277–4688
39 Wang, M. and Thanou, M. (2010) Targeting nanoparticles to cancer. *Pharmacol. Res.* 62, 90–99
40 Zhong, Y. *et al.* (2014) Ligand-directed active tumor-targeting polymeric nanoparticles for cancer chemotherapy. *Biomacromolecules* 15, 1955–1969
41 Mozafari, Z. *et al.* (2019) A novel stimuli-responsive magnetite nanocomposite as de novo drug delivery system. *Polymer Plast. Technol. Mater.* 58, 405–418
42 Jahanban-Esfahlan, R. *et al.* (2020) Dual stimuli-responsive polymeric hollow nanocapsules as 'smart' drug delivery system against cancer. *Polymer Plast. Technol. Mater.* 59 (13), 1492–1504
43 Fathi, M. *et al.* (2020) Therapeutic impacts of enzyme-responsive smart nanobiosystems. *Bioimpacts* 10 (1), 1–4
44 Reyes-Ortega, F. (2014) pH-responsive polymers: properties, synthesis and applications. In *In Smart polymers and their applications*. Elsevier pp. 45–92
45 Tu, Y. *et al.* (2017) Motion manipulation of micro-and nanomotors. *Adv. Mater.* 29 (39), 1701970
46 James, H.P. *et al.* (2014) Smart polymers for the controlled delivery of drugs–a concise overview. *Acta Pharm. Sinica B* 4, 120–127
47 Rao, N.V. *et al.* (2018) Recent progress and advances in stimuli-responsive polymers for cancer therapy. *Front. Bioeng. Biotechnol.* 6, 110
48 De La Rica, R. *et al.* (2012) Enzyme-responsive nanoparticles for drug release and diagnostics. *Adv. Drug Deliv. Rev.* 64, 967–978

49 Kuang, T. *et al.* (2016) Enzyme-responsive nanoparticles for anticancer drug delivery. *Curr. Nanosci.* 12, 38–46
50 Singh, A. and Amiji, M.M. (2018) *Stimuli-Responsive Drug Delivery Systems*. Royal Society of Chemistry
51 Drummond, D.C. *et al.* (2000) Current status of pH-sensitive liposomes in drug delivery. *Prog. Lipid Res.* 39, 409–460
52 Straubinger, R.M. *et al.* (1985) pH-sensitive liposomes mediate cytoplasmic delivery of encapsulated macromolecules. *FEBS Lett.* 179, 148–154
53 Massoumi, B. *et al.* (2020) PEGylated hollow pH-responsive polymeric nanocapsules for controlled drug delivery. *Polym. Int.* 69, 519–527
54 Gauthier, M.A. (2014) *Redox-Responsive Drug Delivery*. Mary Ann Liebert, Inc
55 Huo, M. *et al.* (2014) Redox-responsive polymers for drug delivery: from molecular design to applications. *Polym. Chem.* 5, 1519–1528
56 Men, W. *et al.* (2019) Fabrication of dual pH/redox-responsive lipid-polymer hybrid nanoparticles for anticancer drug delivery and controlled release. *Int. J. Nanomed.* 14, 8001–8011
57 Deatsch, A.E. and Evans, B.A. (2014) Heating efficiency in magnetic nanoparticle hyperthermia. *J. Magn. Magn. Mater.* 354, 163–172
58 Demura, K. *et al.* (2006) An easy-to-use microwave hyperthermia system combined with spatially resolved MR temperature maps: phantom and animal studies. *J. Surg. Res.* 135, 179–186
59 Forbes, N.A. and Zasadzinski, J.A. (2010) Localized photothermal heating of temperature sensitive liposomes. *Biophys. J.* 98, 274a
60 Aryal, M. *et al.* (2013) Multiple treatments with liposomal doxorubicin and ultrasound-induced disruption of blood–tumor and blood–brain barriers improve outcomes in a rat glioma model. *J. Controlled Release* 169 (1–2), 103–111
61 Wang, C. *et al.* (2018) Thermoresponsive polymeric nanoparticles based on poly (2-oxazoline) s and tannic acid. *J. Polym. Sci. Part A: Polym. Chem.* 56 (14), 1520–1527
62 Hribar, K.C. *et al.* (2011) Enhanced release of small molecules from near-infrared light responsive polymer-nanorod composites. *ACS Nano* 5, 2948–2956
63 Geng, S. *et al.* (2017) A light-responsive self-assembly formed by a cationic azobenzene derivative and SDS as a drug delivery system. *Scientific Rep.* 7, 1–13
64 Gerasimov, O.V. *et al.* (1999) Cytosolic drug delivery using pH-and light-sensitive liposomes. *Adv. Drug Deliv. Rev.* 38, 317–338
65 Leung, S.J. and Romanowski, M. (2012) Light-activated content release from liposomes. *Theranostics* 2, 1020–1036
66 Yavlovich, A. *et al.* (2011) A novel class of photo-triggerable liposomes containing DPPC: DC 8, 9 PC as vehicles for delivery of doxorubcin to cells. *Biochim. Biophys. Acta (BBA)-Biomembr.* 1808, 117–126
67 Pradhan, P. *et al.* (2010) Targeted temperature sensitive magnetic liposomes for thermo-chemotherapy. *J. Controlled Release* 142, 108–121
68 Hardiansyah, A. *et al.* (2019) Characterizations of doxorubicin-loaded PEGylated magnetic liposomes for cancer cells therapy. *J. Polym. Res.* 26, 282
69 Halevas, E. *et al.* (2019) Magnetic cationic liposomal nanocarriers for the efficient drug delivery of a curcumin–based vanadium complex with anticancer potential. *J. Inorg. Biochem.* 199, 110778
70 Spizzirri, U.G. *et al.* (2013) Spherical gelatin/CNTs hybrid microgels as electro-responsive drug delivery systems. *Int. J. Pharm.* 448, 115–122
71 Yun, J. *et al.* (2011) Electro-responsive transdermal drug delivery behavior of PVA/PAA/MWCNT nanofibers. *Eur. Polym. J.* 47, 1893–1902
72 Zhao, Y. *et al.* (2016) Nano-engineered electro-responsive drug delivery systems. *J. Mater. Chem. B* 4 (18), 3019–3030
73 Bikram, M. and West, J.L. (2008) Thermo-responsive systems for controlled drug delivery. *Expert Opin. Drug Deliv.* 5, 1077–1091
74 Prabaharan, M. and Mano, J.F. (2006) Stimuli-responsive hydrogels based on polysaccharides incorporated with thermo-responsive polymers as novel biomaterials. *Macromol. Biosci.* 6, 991–1008
75 Van Durme, K. *et al.* (2005) Introduction of silica into thermo-responsive poly (N-isopropyl acrylamide) hydrogels: a novel approach to improve response rates. *Polymer* 46 (23), 9851–9862
76 Zhang, J. and Peppas, N.A. (2001) Molecular interactions in poly (methacrylic acid)/poly (N-isopropyl acrylamide) interpenetrating polymer networks. *J. Appl. Poly. Sci.* 82, 1077–1082
77 Udroiu, I. (2015) Ultrasonic drug delivery in Oncology. *J. Balkan Union Oncol.* 20, 381
78 Ziskin, M.C. (1987) *Applications of ultrasound in medicine—comparison with other modalities. In Ultrasound (XXXX, eds)*. Springer pp. 49–59
79 Chen, H. and Hwang, J.H. (2013) Ultrasound-targeted microbubble destruction for chemotherapeutic drug delivery to solid tumors. *J. Ther. Ultrasound* 1, 1
80 Husseini, G.A. *et al.* (2015) Kinetics of ultrasonic drug delivery from targeted micelles. *J. Nanosci. Nanotechnol.* 15, 2099–2104
81 Kim, H.J. *et al.* (2006) Ultrasound-triggered smart drug release from a poly (dimethylsiloxane)–mesoporous silica composite. *Adv. Mater.* 18 (23), 3083–3088
82 Marin, A. *et al.* (2002) Drug delivery in pluronic micelles: effect of high-frequency ultrasound on drug release from micelles and intracellular uptake. *J. Controlled Release* 84, 39–47
83 Rapoport, N. (2004) Combined cancer therapy by micellar-encapsulated drug and ultrasound. *Int. J. Pharm.* 277, 155–162
84 Xia H. , Zhao Y. , Tong R. (2016) Ultrasound-mediated polymeric micelle drug delivery. Escoffre J.M. Bouakaz A. Therapeutic Ultrasound. Advances in Experimental Medicine and Biology, 880. Springer, Cham. https://doi.org/10.1007/978-3-319-22536-4_20.
85 Nyborg, W.L. (2001) Biological effects of ultrasound: development of safety guidelines. Part II: general review. *Ultrasound Med. Biol.* 27, 301–333
86 Pitt, W.G. *et al.* (2004) Ultrasonic drug delivery–a general review. *Expert Opinion Drug Deliv.* 1, 37–56
87 Zhou, Q.-L. *et al.* (2014) Ultrasound-mediated local drug and gene delivery using nanocarriers. *BioMed Res. Int.* 2014, Article ID 963891 https://doi.org/10.1155/2014/963891
88 Huber, P.E. and Debus, J. (2001) Tumor cytotoxicity *in vivo* and radical formation *in vitro* depend on the shock wave-induced cavitation dose. *Radiat. Res.* 156, 301–309
89 Husseini, G.A. *et al.* (2013) Investigating the acoustic release of doxorubicin from targeted micelles. *Colloids Surf. B: Biointerfaces* 101, 153–155
90 Hangiandreou, N.J. (2003) AAPM/RSNA physics tutorial for residents. Topics in US: B-mode US: basic concepts and new technology. *Radiographics* 23, 1019–1033
91 Bushberg, J.T. *et al.* (2013) In *The Essential Physics of Medical Imaging*. (3rd edn), Wiley
92 Paliwal, S. and Mitragotri, S. (2006) Ultrasound-induced cavitation: applications in drug and gene delivery. *Expert Opin. Drug Deliv.* 3, 713–726
93 Newman, C.M. and Bettinger, T. (2007) Gene therapy progress and prospects: ultrasound for gene transfer. *Gene Ther.* 14, 465–475
94 Pitt, W.G. *et al.* (2004) Ultrasonic drug delivery–a general review. *Expert Opin. Drug Deliv.* 1, 37–56
95 Husseini, G.A. *et al.* (2005) The role of cavitation in acoustically activated drug delivery. *J. Control. Release* 107, 253–261
96 Lohse, D. (2005) Sonoluminescence: cavitation hots up. *Nature* 434 (7029), 33–34
97 Sirsi, S.R. and Borden, M.A. (2014) State-of-the-art materials for ultrasound-triggered drug delivery. *Adv. Drug Deliv. Rev.* 72, 3–14
98 Collis, J. *et al.* (2010) Cavitation microstreaming and stress fields created by microbubbles. *Ultrasonics* 50, 273–279
99 Tzu-Yin, W. *et al.* (2013) Ultrasound and microbubble guided drug delivery: mechanistic understanding and clinical implications. *Curr. Pharm. Biotechnol.* 14, 743–752
100 Izadifar, Z. *et al.* (2017) Mechanical and biological effects of ultrasound: a review of present knowledge. *Ultrasound Med. Biol.* 43, 1085–1104
101 Izadifar, Z. *et al.* (2017) Mechanical and biological effects of ultrasound: a review of present knowledge. *Ultrasound Med. Biol.* 43, 1085–1104
102 Schroeder, A. *et al.* (2009) Ultrasound triggered release of cisplatin from liposomes in murine tumors. *J. Controlled Release* 137, 63–68
103 Brujan, E. (2004) The role of cavitation microjets in the therapeutic applications of ultrasound. *Ultrasound Med. Biol.* 30, 381–387
104 Ohl, S.-W. *et al.* (2015) Bubbles with shock waves and ultrasound: a review. *Interface focus* 5, 20150019
105 Koch, S. *et al.* (2000) Ultrasound enhancement of liposome-mediated cell transfection is caused by cavitation effects. *Ultrasound Med. Biol.* 26, 897–903
106 Lawrie, A. *et al.* (2003) Ultrasound-enhanced transgene expression in vascular cells is not dependent upon cavitation-induced free radicals. *Ultrasound Med. Biol.* 29, 1453–1461
107 May, D.J. *et al.* (2002) Dynamics and fragmentation of thick-shelled microbubbles. *IEEE Trans. Ultrasonics Ferroelectr. Freq. Control* 49, 1400–1410
108 Ter Haar, G. (1990) Biological effects of ultrasound in clinical applications. In *Ultrasound: Its Chemical, Physical, and Biological Effects*, (87) (Suslick, K.S. and Nyborg, W.L., eds) pp. 919–920, ASAJ
109 Martins, S. *et al.* (2007) Lipid-based colloidal carriers for peptide and protein delivery–liposomes versus lipid nanoparticles. *Int. J. Nanomed.* 2, 595
110 Mozafari, M.R. and Khosravi-Darani, K. (2007) An overview of liposome-derived nanocarrier technologies. In *In Nanomaterials and nanosystems for biomedical applications (XXX, eds)*. Springer pp. 113–123
111 Rawat, M. *et al.* (2006) Nanocarriers: promising vehicle for bioactive drugs. *Biol. Pharm. Bull.* 29, 1790–1798
112 Gregoriadis, G. and Florence, A.T. (1993) Liposomes in drug delivery. Clinical, diagnostic and ophthalmic potential. *Drugs* 45, 15–28
113 Pinheiro, M. *et al.* (2011) Liposomes as drug delivery systems for the treatment of TB. *Nanomedicine (Lond)* 6, 1413–1428

114 Vingerhoeds, M. *et al.* (1996) Immunoliposome-mediated targeting of doxorubicin to human ovarian carcinoma *in vitro* and *in vivo*. *Br. J. Cancer* 74, 1023–1029

115 Nkanga, C.I. *et al.* (2019) General perception of liposomes: formation, manufacturing and applications. In *Liposomes: Advances and Perspectives (XXXX, eds), pp. XXX-YYY*. IntechOpen

116 Lattin, J.R. *et al.* (2012) Ultrasound-induced calcein release from eLiposomes. *Ultrasound Med. Biol.* 38, 2163–2173

117 Ninomiya, K. *et al.* (2014) Ultrasound-mediated drug delivery using liposomes modified with a thermosensitive polymer. *Ultrason. Sonochem.* 21, 310–316

118 Schroeder, A. *et al.* (2007) Controlling liposomal drug release with low frequency ultrasound: mechanism and feasibility. *Langmuir* 23, 4019–4025

119 Yan, F. *et al.* (2013) Paclitaxel-liposome-microbubble complexes as ultrasound-triggered therapeutic drug delivery carriers. *J. Controlled Release* 166, 246–255

120 Barenholz, Y. (2002) Cholesterol and other membrane active sterols: from membrane evolution to 'rafts'. *Prog. Lipid Res.* 41, 1–5

121 Jørgensen, K. and Mouritsen, O.G. (1995) Phase separation dynamics and lateral organization of two–component lipid membranes. *Biophys. J.* 69, 942

122 Ta, T. and Porter, T.M. (2013) Thermosensitive liposomes for localized delivery and triggered release of chemotherapy. *J. Controlled Release* 169, 112–125

123 Escoffre, J.M. *et al.* (2013) Doxorubicin liposome-loaded microbubbles for contrast imaging and ultrasound-triggered drug delivery. *IEEE Trans. Ultrason. Ferroelectr. Freq. Control* 60, 78–87

124 Liu, R. *et al.* (2006) The preparation and characterization of gas bubble containing liposomes. *In 2005 IEEE Engineering in Medicine and Biology 27th Annual Conference* 3998–4001

125 Nguyen, A.T. and Wrenn, S.P. (2014) Acoustically active liposome-nanobubble complexes for enhanced ultrasonic imaging and ultrasound-triggered drug delivery. *Wiley Interdiscip. Rev.: Nanomed. Nanobiotechnol.* 6, 316–325

126 Suzuki, R. *et al.* (2008) Effective gene delivery with novel liposomal bubbles and ultrasonic destruction technology. *Int. J. Pharm.* 354, 49–55

127 Novell, A. *et al.* (2015) Focused ultrasound influence on calcein-loaded thermosensitive stealth liposomes. *Int. J. Hyperthermia* 31, 349–358

128 Lin, C.-Y. *et al.* (2014) Ultrasound sensitive eLiposomes containing doxorubicin for drug targeting therapy. *Nanomedicine* 10, 67–76

129 Chen, D. and Wu, J. (2010) An *in vitro* feasibility study of controlled drug release from encapsulated nanometer liposomes using high intensity focused ultrasound. *Ultrasonics* 50, 744–749

130 Zhang, N. *et al.* (2017) Bubble-generating nano-lipid carriers for ultrasound/CT imaging-guided efficient tumor therapy. *Int. J. Pharm.* 534 (1–2), 251–262

131 Staruch, R.M. *et al.* (2015) Hyperthermia-mediated doxorubicin release from thermosensitive liposomes using MR-HIFU: therapeutic effect in rabbit Vx2 tumours. *Int. J. Hyperthermia* 31, 118–133

132 Evjen, T.J. *et al.* (2013) *In vivo* monitoring of liposomal release in tumours following ultrasound stimulation. *Eur. J. Pharm. Biopharm.* 84, 526–531

133 Sirsi, S. and Borden, M. (2009) Microbubble compositions, properties and biomedical applications. *Bubble Sci. Eng. Technol.* 1 (1–2), 3–17

134 Crum, L.A. (1982) Nucleation and stabilization of microbubbles in liquids. *Appl. Sci. Res.* 38, 101–115

135 Miller, D.L. (2007) Overview of experimental studies of biological effects of medical ultrasound caused by gas body activation and inertial cavitation. *Prog. Biophys. Mol. Biol.* 93, 314–330

136 Qin, S. *et al.* (2009) Ultrasound contrast microbubbles in imaging and therapy: physical principles and engineering. *Phys. Med. Biol.* 54, R27

137 Kheirolomoom, A. *et al.* (2007) Acoustically-active microbubbles conjugated to liposomes: characterization of a proposed drug delivery vehicle. *J. Controlled Release* 118, 275–284

138 Fan, C.-H. *et al.* (2013) SPIO-conjugated, doxorubicin-loaded microbubbles for concurrent MRI and focused-ultrasound enhanced brain-tumor drug delivery. *Biomaterials* 34 (14), 3706–3715

139 Hu, J. *et al.* (2016) *In vitro* and *in vivo* evaluation of targeted sunitinib-loaded polymer microbubbles against proliferation of renal cell carcinoma. *J. Ultrasound Med.* 35, 589–597

140 Sun, J. *et al.* (2016) Ultrasound-mediated destruction of oxygen and paclitaxel loaded lipid microbubbles for combination therapy in hypoxic ovarian cancer cells. *Ultrason. Sonochem.* 28, 319–326

141 Fan, C.-H. *et al.* (2016) Ultrasound/magnetic targeting with SPIO-DOX-microbubble complex for image-guided drug delivery in brain tumors. *Theranostics* 6, 1542

142 Wang, C. *et al.* (2017) The anti-tumor effect of folate-targeted liposome microbubbles loaded with oridonin as ultrasound-triggered tumor-targeted therapeutic carrier system. *J. Drug Target.* 25 (1), 83–91

143 Burke, C.W. *et al.* (2014) Ultrasound-activated agents comprised of 5FU-bearing nanoparticles bonded to microbubbles inhibit solid tumor growth and improve survival. *Mol. Ther.* 22, 321–328

144 Burke, C.W. and Price, R.J. (2010) Contrast ultrasound targeted treatment of gliomas in mice via drug-bearing nanoparticle delivery and microvascular ablation. *J. Visual. Exp.* 46, e2145

145 Grainger, S.J. *et al.* (2010) Pulsed ultrasound enhances nanoparticle penetration into breast cancer spheroids. *Mol. Pharm.* 7, 2006–2019

146 Mannell, H. *et al.* (2012) Targeted endothelial gene delivery by ultrasonic destruction of magnetic microbubbles carrying lentiviral vectors. *Pharm. Res.* 29, 1282–1294

147 Shakeri-Zadeh, A. *et al.* (2015) Synergistic effects of magnetic drug targeting using a newly developed nanocapsule and tumor irradiation by ultrasound on CT26 tumors in BALB/c mice. *J. Mater. Chem. B* 3, 1879–1887

148 Beik, J. *et al.* (2016) Nanotechnology in hyperthermia cancer therapy: from fundamental principles to advanced applications. *J. Controlled Release* 235, 205–221

149 Shanei, A. *et al.* (2019) The role of gold nanoparticles in sonosensitization of human cervical carcinoma cell line under ultrasound irradiation: an *in vitro* study. *J. Nano Res.* 59, 1–14

150 Brazzale, C. *et al.* (2016) Enhanced selective sonosensitizing efficacy of ultrasound-based anticancer treatment by targeted gold nanoparticles. *Nanomedicine* 12 (23), 3053–3070

151 Beik, J. *et al.* (2016) Measurements of nanoparticle-enhanced heating from 1 MHz ultrasound in solution and in mice bearing CT26 colon tumors. *J. Thermal Biol.* 62, 84–89

152 Beik, J. *et al.* (2016) Evaluation of the sonosensitizing properties of nano-graphene oxide in comparison with iron oxide and gold nanoparticles. *Physica E: Low-dimensional Syst. Nanostruct.* 81, 308–314

153 Raoof, M. *et al.* (2014) Gold nanoparticles and radiofrequency in experimental models for hepatocellular carcinoma. *Nanomed.: Nanotechnol. Biol. Med.* 10, 1121–1130

154 Xu, Y. *et al.* (2012) Multifunctional magnetic nanoparticles for synergistic enhancement of cancer treatment by combinatorial radio frequency thermolysis and drug delivery. *Adv. Healthcare Mater.* 1, 493–501

155 Wu, S.-K. *et al.* (2014) Short-time focused ultrasound hyperthermia enhances liposomal doxorubicin delivery and antitumor efficacy for brain metastasis of breast cancer. *Int. J. Nanomed.* 9, 4485

156 Han, H. *et al.* (2020) Focused ultrasound-triggered chemo-gene therapy with multifunctional nanocomplex for enhancing therapeutic efficacy. *J. Controlled Release* 322, 346–356

157 Lyon, P.C. *et al.* (2018) Safety and feasibility of ultrasound-triggered targeted drug delivery of doxorubicin from thermosensitive liposomes in liver tumours (TARDOX): a single-centre, open-label, phase 1 trial. *Lancet Oncol.* 19, 1027–1039

158 Kyllönen, H. *et al.* (2005) Membrane filtration enhanced by ultrasound: a review. *Desalination* 181 (1–3), 319–335

159 Sanz Sánchez, I. , Alberto Ortiz-Vigón, A. , Ana Rita Matos, A.R. , David Herrera, D. and Sanz, M. (2011) Clinical evaluation of a protocol of subgingival debridement with Er:YAG laser in comparison to ultrasonic debridement: a randomized clinical trial. In *Proceedings Book Research Session*, HENRY M. GOLDMAN PRIZE https://www.sidp.it/media/taunc8h.pdf

160 Stefanini, M. (2016) *Full Mouth Ultrasonic Debridement: a Therapeutic Protocol for Periodontal Disease Treatment in Patients with Down Syndrome*. 2016 alma

161 Awad, T. *et al.* (2012) Applications of ultrasound in analysis, processing and quality control of food: a review. *Food Res. Int.* 48, 410–427

162 Haupt, G. and Haupt, A. (2003) In vitro comparison of 4 ultrasound lithotripsy devices. *J. Urol.* 170, 1731–1733

163 Guo, S. *et al.* (2011) Tissue ablation using multi-frequency focused ultrasound. *In 2011 IEEE International Ultrasonics Symposium* 2177–2180

164 Barba, F.J. *et al.* (2015) Current applications and new opportunities for the use of pulsed electric fields in food science and industry. *Food Res. Int.* 77, 773–798

165 Gallego-Juárez, J.A. *et al.* (2007) Application of high-power ultrasound for dehydration of vegetables: processes and devices. *Drying Technol.* 25, 1893–1901

166 Khandpur, P. and Gogate, P.R. (2016) Evaluation of ultrasound based sterilization approaches in terms of shelf life and quality parameters of fruit and vegetable juices. *Ultrason. Sonochem.* 29, 337–353

167 Ebenbichler, G.R. *et al.* (1999) Ultrasound therapy for calcific tendinitis of the shoulder. *N. Engl. J. Med.* 340 (20), 1533–1538

168 Zhang, Z.H. *et al.* (2019) Non-thermal technologies and its current and future application in the food industry: a review. *Int. J. Food Sci. Technol.* 54, 1–13

169 Schroeder, A. *et al.* (2009) Ultrasound, liposomes, and drug delivery: principles for using ultrasound to control the release of drugs from liposomes. *Chem. Phys. Lipids* 162 (1–2), 1–16

170 Zhang, J. *et al.* (2018) Ultrasound-triggered drug delivery for breast tumor therapy through iRGD-targeted paclitaxel-loaded liposome-microbubble complexes. *J. Biomed. Nanotechnol.* 14, 1384–1395

171 Geers, B. *et al.* (2011) Self-assembled liposome-loaded microbubbles: the missing link for safe and efficient ultrasound triggered drug-delivery. *J. Controlled Release* 152, 249–256

172 Shore, A. (2018) Retraction: creation of ultrasound and temperature-triggered bubble liposomes from economical precursors to enhance the therapeutic efficacy of curcumin in cancer cells. *RSC Adv.* 8 (69), 39786-39786

173 Wang, C. *et al.* (2017) The anti-tumor effect of folate-targeted liposome microbubbles loaded with oridonin as ultrasound-triggered tumor-targeted therapeutic carrier system. *J. Drug Target.* 25, 83–91

174 Klibanov, A.L. *et al.* (2010) Ultrasound-triggered release of materials entrapped in microbubble–liposome constructs: a tool for targeted drug delivery. *J. Controlled Release* 148, 13–17

175 Prabhakar, A. and Banerjee, R. (2019) Nanobubble liposome complexes for diagnostic imaging and ultrasound-triggered drug delivery in cancers: a theranostic approach. *ACS Omega* 4 (13), 15567–15580

176 Lin, H.-Y. and Thomas, J.L. (2003) Peg-lipids and oligo (ethylene glycol) surfactants enhance the ultrasonic permeabilizability of liposomes. *Langmuir* 19, 1098–1105

177 Lin, H.-Y. and Thomas, J.L. (2004) Factors affecting responsivity of unilamellar liposomes to 20 kHz ultrasound. *Langmuir* 20 (15), 6100–6106

178 De Matos, M.B. *et al.* (2019) Ultrasound-sensitive liposomes for triggered macromolecular drug delivery: formulation and *in vitro* characterization. *Front. Pharmacol.* 10 Article 1463

179 Lin, W. *et al.* (2019) Development and characteristics of novel sonosensitive liposomes for vincristine bitartrate. *Drug Deliv.* 26, 724–731

180 Shalaby, T.I. *et al.* (2020) Smart ultrasound-triggered doxorubicin–loaded nanoliposomes with improved therapeutic response: a comparative study. *J. Pharm. Sci.* 109 (8), 2567–2576

181 Lin, Q. *et al.* (2016) Brain tumor-targeted delivery and therapy by focused ultrasound introduced doxorubicin-loaded cationic liposomes. *Cancer Chemother. Pharmacol.* 77, 269–280

182 Rizzitelli, S. *et al.* (2016) The release of Doxorubicin from liposomes monitored by MRI and triggered by a combination of US stimuli led to a complete tumor regression in a breast cancer mouse model. *J. Controlled Release* 230, 57–63

183 Jeong, H.-S. *et al.* (2016) Effect of high-intensity focused ultrasound on drug release from doxorubicin-loaded pegylated liposomes and therapeutic effect in colorectal cancer murine models. *Ultrasound Med. Biol.* 42, 947–955

184 Kheirolomoom, A. *et al.* (2013) Complete regression of local cancer using temperature-sensitive liposomes combined with ultrasound-mediated hyperthermia. *J. Controlled Release* 172, 266–273

185 Dromi, S. *et al.* (2007) Pulsed-high intensity focused ultrasound and low temperature-sensitive liposomes for enhanced targeted drug delivery and antitumor effect. *Clin. Cancer Res.* 13, 2722–2727

186 Myhr, G. and Moan, J. (2006) Synergistic and tumour selective effects of chemotherapy and ultrasound treatment. *Cancer Lett.* 232, 206–213

187 Treat, L.H. *et al.* (2012) Improved anti-tumor effect of liposomal doxorubicin after targeted blood-brain barrier disruption by MRI-guided focused ultrasound in rat glioma. *Ultrasound Med. Biol.* 38, 1716–1725

188 Yuh, E.L. *et al.* (2005) Delivery of systemic chemotherapeutic agent to tumors by using focused ultrasound: study in a murine model. *Radiology* 234, 431–437

189 Yoon, Y.I. *et al.* (2014) Ultrasound-mediated gene and drug delivery using a microbubble–liposome particle system. *Theranostics* 4, 1133

190 Pitt, W.G. *et al.* (2011) Preliminary results of combining low frequency low intensity ultrasound and liposomal drug delivery to treat tumors in rats. *J. Nanosci. Nanotechnol.* 11, 1866–1870

191 Batchelor, D. *et al.* (2020) Nested-Nanobubbles for Ultrasound Triggered Drug Release. *ACS Applied Mater. Interfaces* 12 (26), 29085–29093

192 Thébault, C.J. *et al.* (2020) Theranostic MRI liposomes for magnetic targeting and ultrasound triggered release of the antivascular CA4P. *J. Controlled Release* 322, 137–148

193 Nittayacharn, P. *et al.* (2019) Enhancing tumor drug distribution with ultrasound-triggered nanobubbles. *J. Pharm. Sci.* 108, 3091–3098

194 Ren, S.-T. *et al.* (2013) The antitumor effect of a new docetaxel-loaded microbubble combined with low-frequency ultrasound in vitro: preparation and parameter analysis. *Pharm. Res.* 30, 1574–1585

195 Deng, Z. *et al.* (2014) Reversal of multidrug resistance phenotype in human breast cancer cells using doxorubicin-liposome-microbubble complexes assisted by ultrasound. *J. Controlled Release* 174, 109–116

196 Liu, H. *et al.* (2014) Ultrasound-mediated destruction of LHRHa-targeted and paclitaxel-loaded lipid microbubbles induces proliferation inhibition and apoptosis in ovarian cancer cells. *Mol. Pharm.* 11, 40–48

197 Escoffre, J.-M. *et al.* (2012) Doxorubicin liposome-loaded microbubbles for contrast imaging and ultrasound-triggered drug delivery. *IEEE Trans. Ultrasonics Ferroelectr. Freq. Control* 60, 78–87

198 Pu, C. *et al.* (2014) Ultrasound-mediated destruction of LHRHa-targeted and paclitaxel-loaded lipid microbubbles for the treatment of intraperitoneal ovarian cancer xenografts. *Mol. Pharm.* 11, 49–58

199 Li, P. *et al.* (2012) Ultrasound triggered drug release from 10-hydroxycamptothecin-loaded phospholipid microbubbles for targeted tumor therapy in mice. *J. Controlled Release* 162, 349–354

200 Ting, C.-Y. *et al.* (2012) Concurrent blood–brain barrier opening and local drug delivery using drug-carrying microbubbles and focused ultrasound for brain glioma treatment. *Biomaterials* 33, 704–712

201 Omata, D. *et al.* (2019) Effects of encapsulated gas on stability of lipid-based microbubbles and ultrasound-triggered drug delivery. *J. Controlled Release* 311, 65–73

202 Kang, J. *et al.* (2010) Antitumor effect of docetaxel-loaded lipid microbubbles combined with ultrasound-targeted microbubble activation on VX2 rabbit liver tumors. *J. Ultrasound Med.* 29, 61–70

203 Tinkov, S. *et al.* (2010) New doxorubicin-loaded phospholipid microbubbles for targeted tumor therapy: Part I—formulation development and in-vitro characterization. *J. Controlled Release* 143, 143–150

204 Hijnen, N. *et al.* (2017) Thermal combination therapies for local drug delivery by magnetic resonance-guided high-intensity focused ultrasound. *Proc. Natl. Acad. Sci. U.S.A.* 114 (24), E4802–E4811

205 de Smet, M. *et al.* (2011) Magnetic resonance imaging of high intensity focused ultrasound mediated drug delivery from temperature-sensitive liposomes: an *in vivo* proof-of-concept study. *J. Controlled Release* 150, 102–110

206 Patel, P.R. *et al.* (2008) *In vitro* and *in vivo* evaluations of increased effective beam width for heat deposition using a split focus high intensity ultrasound (HIFU) transducer. *Int. J. Hyperthermia* 24, 537–549